A Visual Analytics Process for Exploring Risk and Vulnerability in International Food Trade Networks

by

Travis Seville

A Thesis Presented in Partial Fulfillment
of the Requirements for the Degree
Master of Science

Approved November 2017 by the
Graduate Supervisory Committee:

Ross Maciejewski, Chair
I-Han Hsiao
Shade Shutters

ARIZONA STATE UNIVERSITY

December 2017

ABSTRACT

The rise in globalization has led to regional climate events having an increased effect on global food security. These indirect first- and second-order effects are generally geographically disparate from the region experiencing the climate event. Without understanding the topology of the food trade network, international aid may be naively directed to the countries directly experiencing the climate event and not to countries that will face potential food insecurity due to that event. This thesis focuses on the development of a visual analytics system for exploring second-order effects of climate change under the lens of global trade. In order to visualize how climate change impacts the world trade network of agricultural goods I have developed an interactive data visualization platform for analysis of the interaction between climate events and the trade network. The proposed visual analytics system focuses on visualizing current trade dependencies at a more granular level than the currently available tools and to aid in the identification of future vulnerabilities. To demonstrate the applicability of the tool, two case studies are described. The first case study focuses on the Chinese drought of 2011 and its impact on the global trade network and food security. The second case study will model the potential impact of a climate event affecting production in the United States, a large supplier of corn, to demonstrate the potential consequence of cascading effects in the global trade network.

I dedicate this thesis to my family; for their support and consistent motivation.

My parents. Without them, none of this would have been possible.

My wife, Nichole, who pushed me and always held me accountable.

My children, Lacy, Lia and Logan, who inspired me.

TABLE OF CONTENTS

CHAPTER Page

LIST OF TABLES

LIST OF FIGURES

Chapter 1

INTRODUCTION

Currently, limited research has focused on the inspection of the international food trade network taking into account second-order effects of climate events on the food trade network. These second-order effects are generally geographically disparate from the first-order effects and frequently affect poorer areas that are less capable of dealing with the change, i.e. countries at a higher risk of food insecurity. From my literature study, previous research has summarized this data but has not allowed for a real-time exploration of the international food trade network.

This thesis presents a visual analytics system that showcases the indirect effects of a climate event. The region that originally experienced the climate event is generally well recognized and modeled. This tool improves on the current analysis techniques by cascading the consequences of the climate event downstream along the food trade network. This has the potential to identify the level of vulnerability of a country affected by the second-order effects of a climate event. The goal here is to mitigate food security concerns before they result in larger issues by affecting policy and redirecting international aid or development from the climate change event stricken country to the food security affected country. The dashboard will merge the related areas of the international food trade network, climate change, and food security into a visual representation of vulnerability.

Such analyses are especially critical as more globalization has occurred. Our goal is to give decision makers an awareness of the role that networks play in food, water and political vulnerability. Such work is key to identifying potential cascading impacts of climate change. Examples of such cascading effects include the recent Arab Spring

movement which has has been linked to an increase in cereal prices by a number of studies (Johnstone and Mazo (2011), Sternberg (2012)). These social and economic disruptions were not a direct result of under-production in Egypt or the Middle East but likely due to trade disruptions. These disruptions were prompted by a sharp drop in wheat production in China. Studies suggest that China was forced to import more wheat to feed their people, resulting in markets driving an increase in wheat prices and market uncertainty prompting continued export bans in certain countries (Fellmann *et al.*, 2014). Simply put, a regional climate event in China (the 2011 drought) potentially had a global effect on food security.

Thus, food production increases to meet global demand and climate events are becoming increasingly more destructive. In 2005 Hurricane Katrina struck the Gulf Coast region and left far-reaching destruction. The Farm Bureau estimates direct farm production losses to be $1 billion dollars and another $1 billion in indirect costs (Schnepf and Chite, 2005). This is just one example of a climate singularity having a direct impact on agricultural production, and recent studies indicate growing climate concerns. For example Webster *et al.* (2005) and Trenberth (2005) agree that although there is not defined statistical evidence of an increase in the number of cyclones, there was evidence of an increase in the intensity of the storms, which can lead to increased devastation.

There is no doubt that climate change will adversely affect food security and will increase the import dependency of developing countries (Schmidhuber and Tubiello, 2007). As more extreme events occur due to climate change, more supply shocks will arise. The intensification of climate extremes is predicted to increase the variability and uncertainty of crop yields (Stocker *et al.*, 2013). Thus climate change has major repercussions on the health of the international food trade network and global food security. As such, we need new methods to study the cascading impacts of climate

events.

One means of looking at the cascading effect of climate change is to analyze the international food trade network. The food of almost a billion people is produced outside their countries (Fader *et al.*, 2013) and imported. This is only possible as a result of the international food trade network. There has been a recent surge in international trade as water poor countries rely more heavily on the global food supply system and are more vulnerable to price fluctuations. Food crises are not a new thing. An example of this is the food crises of 1972/1973. The crisis was the result of a large scale el Nino event affecting production and policies enacted by the United States and the Soviet Union (Timmer, 2010). Thailand was the world's leading rice exporter at the time and for nine months during the crises implemented an export ban effectively wiping out the world rice market. When Thailand lifted that ban their rice prices had quadrupled.

In 2007/2008, the cereal price index reached a peak 2.8 times higher than in 2000 (UNDESA, 2011). In 2010/2011 wheat prices jump from $4 to $9 a bushel in less than seven months. In Egypt wheat prices doubled and the price of bread tripled (Sternberg, 2012). Rioting in Algeria, Tunisia and Egypt was a direct response to higher prices for wheat and bread (Johnstone and Mazo, 2011). Studies have indicated that excessive import dependence is a risk factor of food insecurity (Fader *et al.*, 2013) and supply shocks downstream of major exporters are a concern (Gephart *et al.*, 2016). When these trade links are perturbed it can pose a major risk to food security by transferring vulnerability from one country to another.

In order to explore and understand these vulnerabilities, this thesis develops a visual analytics system to explore network dependencies for analyzing potential impacts to the international food trade network and food insecurity due to climate events. First, the international food trade network is modeled as a weighted directed

network graph. The nodes of this network graph are the countries and the edges are trade links between the countries. The edges are weighted by the import dependence of that particular agricultural good. Climate events are simulated with an export reduction paradigm; the region experiencing a climate event reacts to it by reducing the amount of trade goods they export. The amount reduced could be due to a direct crop-production reduction, a policy effect such as an export ban or reduction, or a combination of both. The result of this export reduction is cascaded along the food trade network; countries whose imports are directly affected by the export reduction reduce their own exports to mitigate the loss of imports. This is how the effects are effectively cascaded down the food trade network. The potential for food insecurity is then visualized in a choropleth representing the calculated vulnerability index based on the scenario parameters provided.

The use of this visual analytics system in this thesis has been catered to appreciate the effects of a climate event. However, the basis for simulation is the export reduction paradigm, which is not limited in scope to climate events. As this system maps vulnerability based on the reduction in imports received, it is independent of climate or food and therefore is able to handle different types of trade goods. In the case studies presented here the vulnerability directly maps to food insecurity, but there is no reason the system could not be utilized to monitor dependency on other critical goods, such as raw materials for manufacturing. Thus, this system has the potential to be used independent of food security or climate change and events.

In Chapter 2 a literature study is conducted and relevant works are reviewed. Chapter 3 illustrates the system architecture. The 2011 Chinese drought is explored along with a simulation case study in Chapter 4. Finally, Chapter 5 summarizes this work.

Chapter 2

RELATED WORK

This thesis presents a visual analytics system to analyze risk and vulnerability based on the impacts to the international food trade network due to direct and cascading effects of a climate event. Current visualization tools in the area of climate change and the food trade network are examined. There are a number of relevant fields that are reviewed to understand these effects including the international food trade network, network graphs and visual analytics. Previous work on the topic of the food trade network, its composition and dependencies, is reviewed. As the food trade network is modeled as a network graph in this system, previous work on network graphs is reviewed. Lastly in order to present the system in an effective manner related work in the field of visual analytics is reviewed.

2.1 Existing Visualizations

A number of visualization systems have been developed to enable the exploration of food security, trade and climate change. I reviewed these systems and found a number of limitations related to this thesis. The general limitation of these systems is that the food trade network and food security indices are not modeled together and their interaction and analysis capabilities are limited in scope.

Climate change models and future food insecurity index forecasts are visualized on the *Food Insecurity and Climate Change* website (Figure 2.1), hosted by the Met Office and World Food Programme. The website allows users to explore different scenarios of adaptation to climate change and greenhouse gas emissions. The visualization presents a long range (2050s and 2080s) forecast of the potential for food

insecurity based on these factors. However, the visualization does not consider the food trade network at all and does not allow for any simulation of specific climate events, preventing the use as a directed analysis tool.

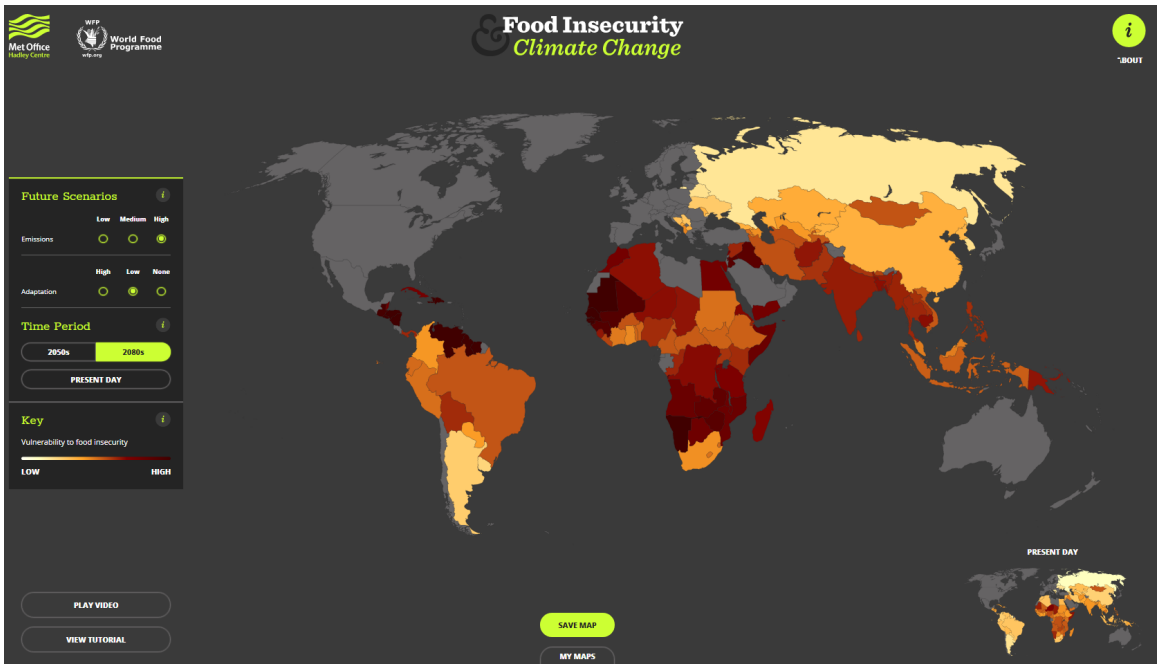

Figure 2.1: Met Office Food Insecurity & Climate Change website (www.metoffice.gov.uk/food-insecurity-index). The Met Office is the United Kingdom's national weather service. Their visualization shows a measure of how vulnerable a country's food security system is to the negative impacts of weather and climate (Hadley Center, 2017). The darker red colors indicate a higher level of vulnerability. Future scenarios allow for predictions based on the options selected. The current display shows the vulnerability to food insecurity for the 2080s based on a scenario of high emissions and low adaptation levels.

Trade data can be visualized directly on the FAOSTAT website as seen in figure 2.2. This data visualization takes one country and displays the import or export trade links of a single trade good for that country. The visualization is done as a geographic choropleth representing the quantity or value of the imported or export good to another country. However, the visualization is ineffective as it only displays a single country's import or export contribution. It does not take into consideration the food trade network as a whole and does not allow for any interactions. These

limitations again preclude any use for analyzing the effects of a change to the food trade network.

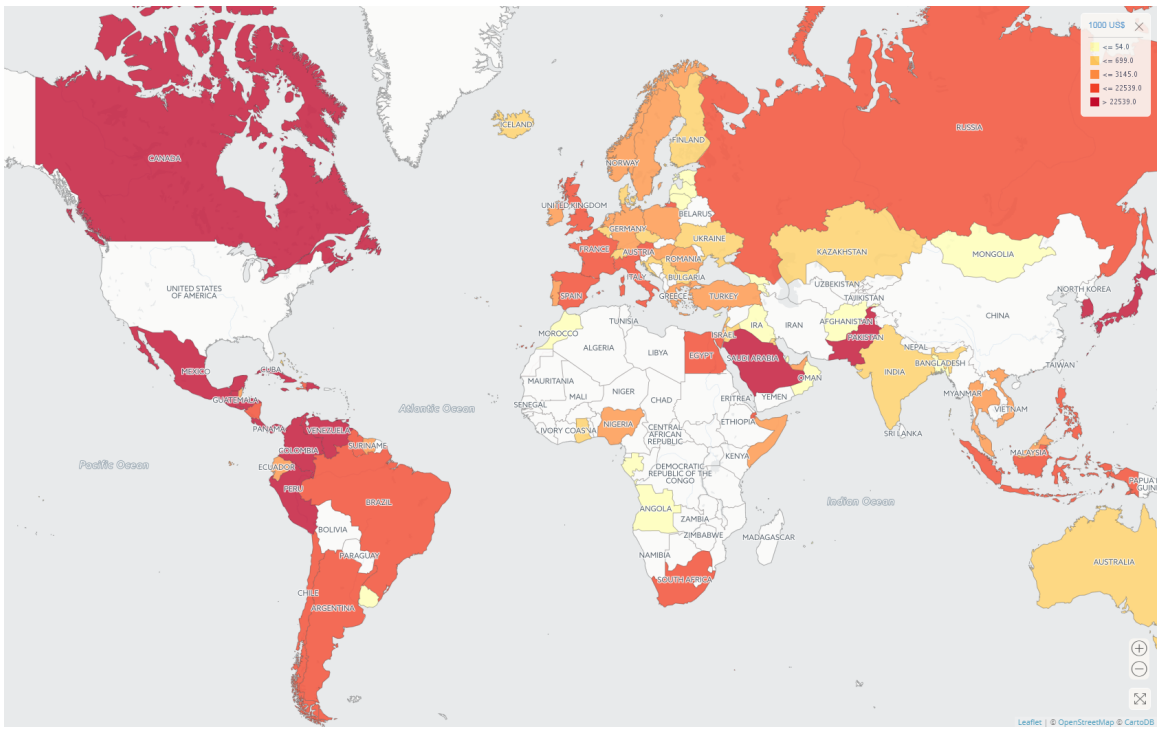

Figure 2.2: FAOSTAT data visualization website (www.fao.org/faostat/en/#data/TM/visualize). The FAOSTAT is Food and Agriculture Organization of the United Nations Statistics Division. Their system shows the value of import or export trade links to or from the selected country for the given time period in a choropleth. The current display shows the dollar value of corn exported by the United States in the year 2013. The darker red the color a country is colored, the more the United States exported to that country.

2.2 Trade Networks and Food Security

The increase of globalization has led to a marked decrease in the proportion of hungry people globally (Godfray *et al.*, 2010). The international food trade network is used to feed people that were traditionally reliant on domestic production. Given that countries are becoming increasingly more import dependent (D'Odorico *et al.*, 2014), the effects of disruptions to the food trade network are magnified. Kali and Reyes (2007) suggest that a network approach considering the cascading of shocks

will be invaluable.

Headey (2011) highlights recent food crises and associates them to disruptions in the international food trade network due to surges in cereal prices. The cereal price surge in 2007 and 2008 is explored with an emphasis on how four staple good markets were negatively affected, leading to food security issues. Export restrictions and droughts were a major player in the volatility of the international food trade network at the time. According to (Brobakk and Almås, 2011), uncertainty in markets can lead to export bans which can lead to food insecurity. These works help provide understanding of the interaction between the trade network and food insecurity.

The food trade network can also be a tool to help deal with food security issues. Most of the global population is a resident of a net food importing country and so not self-sufficient, concluding that the world has moved from food insufficiency to an increasing food trade dependency (Porkka *et al.*, 2013). This is especially true in the Middle East. The majority of Arabic countries import more than 50% of their caloric intake (FAO, 2016). Suppliers are limited, with five exporters (Argentina, Australia, Canada, the European Union and the United States) accounting for almost three-quarters of the world's traded staple crops (FAO, 2016). d'Amour *et al.* (2016) classifies countries vulnerability based on their level of caloric trade dependency. High dependency on a single staple crop for supply of calories and a high dependency on imports indicates a higher risk. This model of risk is used as the basis for the vulnerability index in this thesis.

Identified vulnerable countries also receive their imports from just a few dominant producing countries. Silberglitt (2015) explains the concern of two-tier pricing involved in concentrations of producers. Producers are able to influence the pricing on the market by enforcing export restrictions or bans, resulting in preferential domestic supplies. This has the potential of exacerbating the effects of a supply-side

shock, which can be devastating to the entire food trade network. Exposure to non-domestic supply shocks is a trade-off to an increasingly globalized food trade network. According to Gephart *et al.* (2016), exposure to this risk can be reduced by a diverse trade portfolio. These supply shocks are one representation of the cascading effects of a climate event.

An example of a supply shock by a major exporter is reviewed in Fellmann *et al.* (2014). Russia, Ukraine and Kazakhstan temporarily placed export bans on wheat following poor harvest due to drought. This shows that shocks affecting more network-central countries are more likely to be transferred to other areas of the network. Net grain importing countries are at a major risk when diverse import trade portfolios are not present. This previous work provides the basis for my first case study.

The value of a link in the food trade network can be represented in many fashions. MacDonald *et al.* (2015) suggest that in the modern era of globalization it may be more beneficial to think of a product's values using a resource metric such as cropland area. Monetary value can change with a number of factors and is so discouraged. Another useful metric we discovered may be calories or virtual water. Expanding on the concept of virtual water Hoekstra and Hung (2005) quantifies the calculations of water demand for specific crops. Virtual water balances are defined as the difference of gross virtual water imports and exports. Developed countries tend to have a more stable virtual water balance. Knowledge of the national virtual water balance is important in policy development because water scarcity is a driver of international food trade. Konar *et al.* (2011) explores the virtual water trade network as a amalgamation of the international food trade network. The topic provides a framework for use of water trade as the network model. Network graph statistics are produced for the virtual water representation of the international food trade network. Dominant countries are highly connected and are identified as hubs which connect to

the large number of small trade-volume countries. Hoekstra and Mekonnen (2012) introduces water footprints and illustrates the global dimension of water consumption and pollution by showing that several countries heavily rely on foreign water resources. Many countries have significant impacts on water consumption and pollution elsewhere. Policies in this context translate to food security concerns and water footprints should be understood for development of these policies. This also solidifies the relationship between climate events, which generally affect water availability, and the food trade network. Because of increased globalization climate events are no longer localized and these regional events may have global effects on food security (Sternberg, 2012), validating the need for this second-order effect model.

Related work in the area of the international food trade network provides the preliminary domain-knowledge required for the effective development of a related visual analytic system. With understanding of the interactions and consequences of perturbations to the food trade network I was able to more effectively model the food trade network's cascaded effects. The literature reviewed here allowed for the connection between food insecurity vulnerability and the food trade network.

2.3 Network Graphs

To accurately model cascading effects we need to understand the topology of the international food trade network when represented as a node-edge graph. Serrano and Boguná (2003) states the world trade network has become a self-organized complex system that must be considered in its entirety.

The international food trade network is essentially a very dense network graph and can be modeled as $G = (V, E, W, T)$. V is the set of vertices, represented by all the countries involved in the food trade network. E is the set of trade links, defined $E_n = \{V_i, V_j, t\}$. Direction is indicated with the importing country represented by

$V_i \in V$ and the exporting country, $V_j \in V$. T is the set of all trade goods. The good represented by an edge is $t \in T$. The weight of the edge is the defined as the function $w_{i,j,t}$. The weight function is the dollar value of the trade link of the specified good from country j to i. The number of nodes is limited to the number of countries involved but the number of edges is extraordinary due to the large number of goods being traded and the number of unique trade partners.

Subgraphs are pieces of more complex networks and specifically three node subgraphs are labeled as triads. Milo *et al.* (2002) classifies these subgraphs occurring a significantly higher rates than expected as motifs. There are examples of motifs found in biological (Shen-Orr *et al.*, 2002), technological (Milo *et al.*, 2002) and agricultural (Shutters and Muneepeerakul, 2012) networks. The recurrence of these motifs show patterns that occur much more frequently in real networks than in randomized networks. This indicates that a structure exists which can be classified. A number of different classifications are presented and motif frequencies are examined for those distinct types. These network motifs are discovered here and also in Grochow and Kellis (2007). This introduces a novel approach for motif discovery that utilizes a method for searching for a single network motif as opposed to enumerating subgraphs. It also takes advantage of symmetry of motifs to reduce the number of iterations. Stouffer *et al.* (2012) contains information on the different unique motif positions. This provides the reference when identifying the positions as well as the triad numerical classification. There are between one and three different unique motif positions depending on the type and thirty different unique positions over the thirteen different triads. The number and type of motifs in a network are important characteristics that directly affect stability of the network. The usefulness of using a reciprocal model for determination of the type of triad is confirmed in Squartini and Garlaschelli (2012). Models should take into account not only in the in and out

degrees of the motifs but also the reciprocity of the links. With this representation the model can replicate the triadic structure. This suggests the dyadic structure of the network is information rich. Zhou *et al.* (2016) employs a model that uses country behavior in the local triadic environment to account for the formation of such network structure. Different network graphs are created based on a country's top one or two trading partners. These truncated network graphs are shown to extract the more important information of the network. In this system these classifications of subgraphs are used to construct the triads.

Triad significance profiles (TSP) are an area of emerging research where the prevalence of certain triads is compared to normal distributions. Winkler and Reichardt (2013) produces generative models that would create network graphs based on these triadic z-score profiles. Shutters and Muneepeerakul (2012) lays the groundwork for association of triad significance profiles in the international food trade network to economic health. There are similarities of agricultural trade network with known triad significance profile of human social networks and biological information processing networks to a lesser degree. Superfamilies of existing networks are compared against the international food trade network and a distinct superfamily for the food trade network is identified. My framework visualizes these TSP for potential association to food trade network health.

Other related works focus on the international food trade network's specific network graph statistics Fagiolo *et al.* (2010) and topology (Serrano and Boguná, 2003). The density of the network graph as indicated by Schiavo *et al.* (2010) shows that there is a high level of clustering and that the topology of the international trade network is indeed important. Three data points for nodes are defined; node degree (the number of links maintained by each node), average nearest neighbor degree (the correlation between the degree of a node and the average degree of its partners) and

clustering coefficient (the percentage of pairs of a node's partners that are connected among themselves). Importance should be given to the distribution of trade links across all trade partners. Kali and Reyes (2007) explains that a country's position in the network has substantial implications for quantifying economic growth. The majority of countries involved in the trade network are characterized by weak links, with a small number of countries exhibiting strong relationships indicating a core-periphery structure. The clustering coefficient is high in the international food trade network and has a high level of centralization, implying a hierarchical structure as suggested in other research (Zhou *et al.* (2016), Garlaschelli and Loffredo (2005)). Zhou *et al.* (2016) constructs the network based on the top trade links and indicates there is indeed a hierarchy. (Ravasz and Barabási, 2003) and (Zhou *et al.*, 2016) show that real networks are not randomized, but follow a pattern of organization related to hierarchy. At higher levels of trade, the network is considered scale-free; there is no typical country in terms of number of trading partners. The properties of scale-free networks are examined in Li *et al.* (2005). The power law degree distributions of the international food trade network align with these observations.

As the international food trade network was modeled as a network graph, the literature reviewed here allowed for an effective understanding of the underlying construction. The dependencies in the food trade network are related to the topology of the network graph. Although TSP analysis was passed in favor of a cascading effect model the foundation for future work is established with the related work here.

2.4 Visual Analytics

Visual analytics has become the preferred tool for domain-experts exploring large data sets. It is defined by Cook and Thomas (2005) as "analytical reasoning facilitated by interactive visual interfaces." Shneiderman (1996) introduces the well-known

information seeking mantra: overview first, zoom and filter, then details-on-demand. Visual analytics, per Keim *et al.* (2006), extends this mantra to include the combination of data analysis and interactive visual interfaces: "analyze first, show the important, zoom/filter/analyze further and details on demand."

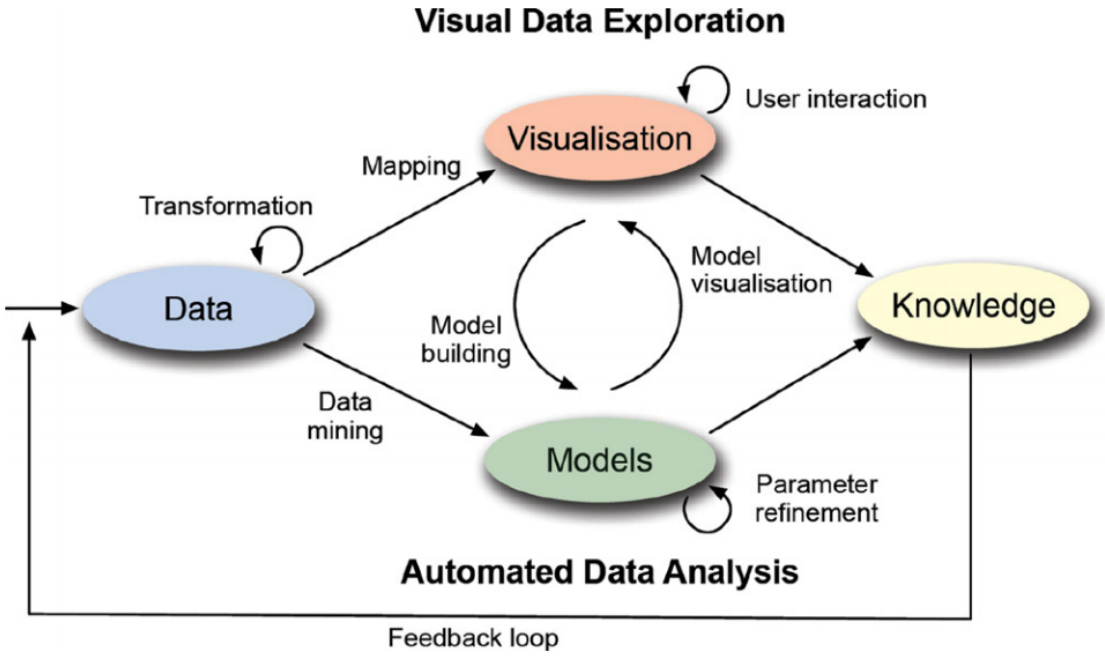

Figure 2.3: Visual Analytics Framework, (Keim *et al.* (2008), Keim *et al.* (2011))

Keim *et al.* (2008) introduces the framework for visual analytics (Figure 2.3). The framework captures the process of a typical sense-making session. First, data is transformed by filtering and models are built from the resultant data subset. Visual data exploration is then applied with interactive visualizations to analyze and explore the data. Automatic analysis is done at each iteration of a feedback loop to produce results. The feedback loop helps repeat this process until sufficient refinement of the results is achieved. This automated analysis techniques were used by this thesis to calculate vulnerability indices after each iteration of the feedback loop.

To build the visual analytics system, the first step is data analysis. Previous research (Zhou *et al.* (2016), Shutters and Muneepeerakul (2012), Squartini and Gar-

laschelli (2012)) has provided some initial data analysis that is supplemented by our own resources. Triads are calculated, motif positions are generated and bilateral trade links are computed. Further analysis is accomplished by the user interaction and filtering of interesting data in the feedback loop.

The next step is analysis via interactions with the visualizations. In visual analytics involving graphs, Sun *et al.* (2013) shows recent research has focused on the visual mapping aspect of the analytics systems over the model-based analysis. Graph data is highly structured and is a possible reason for this paradigm.

Visualizing a network graph can be done in two primary ways: node-link diagrams and adjacency matrices. The most familiar visualization is the node-link diagram . Ghoniem *et al.* (2004) considers the two different representation and compares the readability of the two graphs. Although the international trade network starts out with a large number of nodes, when filtering is applied (Shneiderman, 1996) it has a limited number of nodes. Therefore when choosing the appropriate visualization I consider it a small graph, and node-link diagrams are more readable (Ghoniem *et al.*, 2004).

Node placement is a consideration when network visualization is concerned. A common layout strategy is based on geographic representation (Shneiderman and Aris, 2006). This geographically representative positioning is used in both of the main visual representations. The linked multiple views of the familiar world map (choropleth) and the network visualization allow for a greater understanding (Rodgers, 2005) and allow for mental mapping (Eades *et al.*, 1991).

When visualizing a network minimizing edge crossing is the most important aesthetic consideration (Purchase, 1997) for improving human comprehension. A number of different algorithms for graph visualization were reviewed (Herman *et al.* (2000), Dunne and Shneiderman (2013), Holten and Van Wijk (2009)) that help with this

consideration. Herman *et al.* (2000) overviews a number of basic graph layout algorithms in the context of information visualization. Dunne and Shneiderman (2013) offers a technique to simplify highly clustered network graphs by aggregating subnetworks. Simplifying the drawing of certain types of motifs can greatly increase readability in dense network graphs. Holten and Van Wijk (2009) shows another example of a technique aimed at simplifying complex network graphs. This is achieved by bundling of similarly drawn edges and subsequent splitting of the edges closer to the termination node. Ultimately these algorithms were removed from consideration in favor of mental mapping (Eades *et al.*, 1991) and interpretability (Keim *et al.*, 2008). Nodes were positioned approximately geographic to aid in the establishment of this mental map. The minimization of edge crossing is accomplished interactively by dragging of nodes after a simulation baseline is established.

The parameters for the algorithms are usually considered in multiple solutions before results are achieved (Hund *et al.*, 2016). In this system the reasoning is done by the human analyst (Andrienko *et al.*, 2011), and the interaction allows for the parameters of the algorithms to be manipulated by the users.

Knowledge in this field was pertinent to the development of effective human computer interaction techniques used in this system. The visual analytic paradigm providing for the feedback loop was implemented to allow for analysis of the effects of a simulated climate event.

The work reviewed here provides the framework for my visual analytic system. I build the framework on the principles defined in the visual analytics mantra (Keim *et al.*, 2006). The representation of the network graph as a node-link diagram instead of an adjacency matrix was based on the suggestions of previous research included in this section. The visual design was also inspired by the mental mapping paradigm.

Chapter 3

SYSTEM

The goal of the proposed visual analytic system is to enable analysts to simulate the first- and second-order effects of climate events to the food trade network. Identification of the effects, along with potentially vulnerable countries, can be used by policy makers and international aid managers. For instance, in the event of a drought in Argentina, analysts would be able to use the framework to determine which countries would likely be impacted the most. They could then advise international aid managers to begin staging supplies near the predicted areas.

3.1 Data, Assumptions, and Formulas

The Food and Agriculture Organization (FAO) of the United Nations (UN) Statistics Division maintains the Food and Agriculture Organization Corporate Statistical Database (FAOSTAT). This database provides free access to food and agriculture data for over 245 countries and territories and covers all FAO regional groupings from 1961 to the most recent year available (FAO (2016)).

The data in this thesis is a snapshot from the FAOSTAT database containing trade link data for the years 1986 through 2013. The FAOSTAT database contains a reporting country, a partner country, the type (i.e. import or export), the trade year, the trade good and dollar value. A country will report the value of a particular good it imported for that year from the partner country. That partner country also reports the exporting value. Since these two reports are not always the same, as seen in Table 3.1, some preprocessing is required.

Trade Year	Reporter	Partner	Type	Item	Value
2011	USA	Japan	Maize	Export	$3,831,683,000
2011	Japan	USA	Maize	Import	$4,818,714,000

Table 3.1: Sample FAOSTAT data

Since the FAOSTAT database contains two sets of data, the importing country's reported data and the exporting country's reported data, preprocessing was done to merge the two reported values. The processed trade links are then defined by the exporting country, the importing country, the trade year, the trade good and the dollar value of the trade link. Some example links are shown in Table 3.2. Bilateral trade associations and triad constructions were calculated and stored in our database.

Trade Year	Exporter	Importer	Item	Value
2011	USA	Japan	Maize	$4,325,199,000
2011	Poland	Sweden	Molasses	$2,648,000
2011	Afghanistan	Australia	Almonds shelled	$13,000

Table 3.2: Sample trade links comprising the international food trade network

To model the cascading effects of a climate event a simulation engine was created. In construction of the simulation engine we made the following assumptions. First, for the simulation of a climate event, the trade link value for all the selected country's export links is reduced. For instance, if a 10% reduction in wheat exports is simulated from a country, every export trade link is reduced by 10%. Second, the reduction percentage is a reduction of export links and not a reduction of production. This is important because if a production reduction is assumed it could potentially decrease

the export trade links by a larger amount than the specified reduction for the country to maintain its own stores of the trade good. Another benefit is that we are able to model indirect export reductions, such as export restrictions. Third, the export links will all be reduced regardless of outside influences. There is no favoritism in the decision making of which export trade links to reduce; that is, there is an equal reduction in trade goods to all trading partners. Lastly, the reduction in imports to a country is then extrapolated to its own export trade links. The country is calculated to lose that value of goods and will first reduce its own exports to mitigate the loss of imports. Such assumptions pose the risk of an overly simplistic export reduction formula which may not be realistic, however we believe that it does offer a good starting point.

The vulnerability index to a country is then defined as

$$v = \frac{\sum_I - \sum_{I_\Delta}}{\sum_I + \sum_E} \tag{3.1}$$

where $\sum_I$ is the sum of the country's import trade links dollar values before the simulation reduction, $\sum_{I_\Delta}$ is the sum of all of the country's import trade link dollar values after the simulation reduction and $\sum_E$ is the sum of all of the country's export trade link dollar values before the simulation reduction. Note that denominator is the sum of both import and export trade link dollar values. Again, we make the assumption that a country would reduce its exports to overcome the loss of imports.The range of values is 0 to 1 and a higher number indicates a higher vulnerability. If a country does not suffer any import reduction, that is $\sum_{I_\Delta} = \sum_I$, then the vulnerability index will be 0: $v = 0$. If a country loses its entire import portfolio, that is $\sum_{I_\Delta} = 0$, the vulnerability index is then a function of the value of its ratio of its imports and exports: $\frac{\sum_I}{\sum_I + \sum_E}$. If that country does not have any export links, that is $\sum_E = 0$, then the vulnerability index is a function of the value of lost imports: $\frac{\sum_I - \sum_{I_\Delta}}{\sum_I}$. If a

country does not have any export links and loses its entire import portfolio, that is $\sum_E = 0$ & $\sum_{I_\Delta} = 0$, then the vulnerability index will be 1: $v = 1$.

Another index used in the system is import dependence, defined as

$$d_l = \frac{l}{\sum_I + \sum_E} \tag{3.2}$$

where l is the dollar value of the trade link and $\sum_I$ is the sum of the all of the country's import trade link dollar values and $\sum_E$ is the sum of the all of the country's export trade link dollar values. The higher the number the higher the import dependency of the trade link. Note that denominator is the sum of both import and export trade links. Again, we make the assumption that a country would reduce its exports to overcome the loss of imports.

3.2 System Architecture

The proposed visual analytics system is a web-based system consisting of a front-end website for user display and interaction and a back-end system for data retrieval. The system is accessible from a modern web browser and was developed with an HTML front-end utilizing JavaScript for advanced features. The core of the visualization was created by an open-source JavaScript library called Data-Driven Documents (D3), (Bostok, 2016). This is a JavaScript library providing many mechanisms for manipulating document object model (DOM) elements based on data. A powerful concept which was utilized extensively was selections. This allows attribution of an array of data to an element, usually a DIV. Then child nodes are created, updated, and destroyed based on changes to the array. This mechanism allowed a extremely large dataset to be held in memory. The benefits of this are two-fold; efficient manipulation of the dataset resulting in responsive visualizations and reducing the need for numerous database calls limiting the effect of network latency.

Connecting the front-end to the back-end are RESTful APIs. The APIs exist on the back-end web servers to connect to a database and provide the data to the front-end. These APIs were written in Java and utilize a mechanism to execute simple transactional-SQL queries. The data is then returned in a D3 friendly arrayed JavaScript Object Notation (JSON) formatted object for processing in the front-end.

3.3 Visual Analytics Framework

A diagram of the visual analytic framework is shown in Figure 3.1. The three parts of the system are the data, the model and the visualization. In my system the data is the database and supplemental data as described in Section 3.1. The model part of the system is accomplished by modeling the trade links as a network graph and calculation of vulnerability indices, triad z-scores and import dependencies. These calculations are described in more detail in the following sections. The visualization graphically represents the data and models to allow for analysts to visually detect patterns. The feedback loop is made up of the action and finding boxes on the right side of Figure 3.1.

My framework allows for a domain expert to simulate a climate event to explore the first- and second-order effects to the international food trade network and identify any potentially vulnerable countries. After a subset of data is selected, a simulation is modeled and the visualization displays the effects. Further filtering and interactions, such as panning and zooming, in the feedback loop allow for enhanced pattern recognition.

The main visualization of the visual analytic system is a dashboard (Figure 3.2). In the top left part of the dashboard a combo box exists so the user may select the year to analyze. The rest of dashboard is composed of 5 distinct sections as seen in Figure 3.2. The histogram charts in Figure 3.2-1 shows the distribution of trade

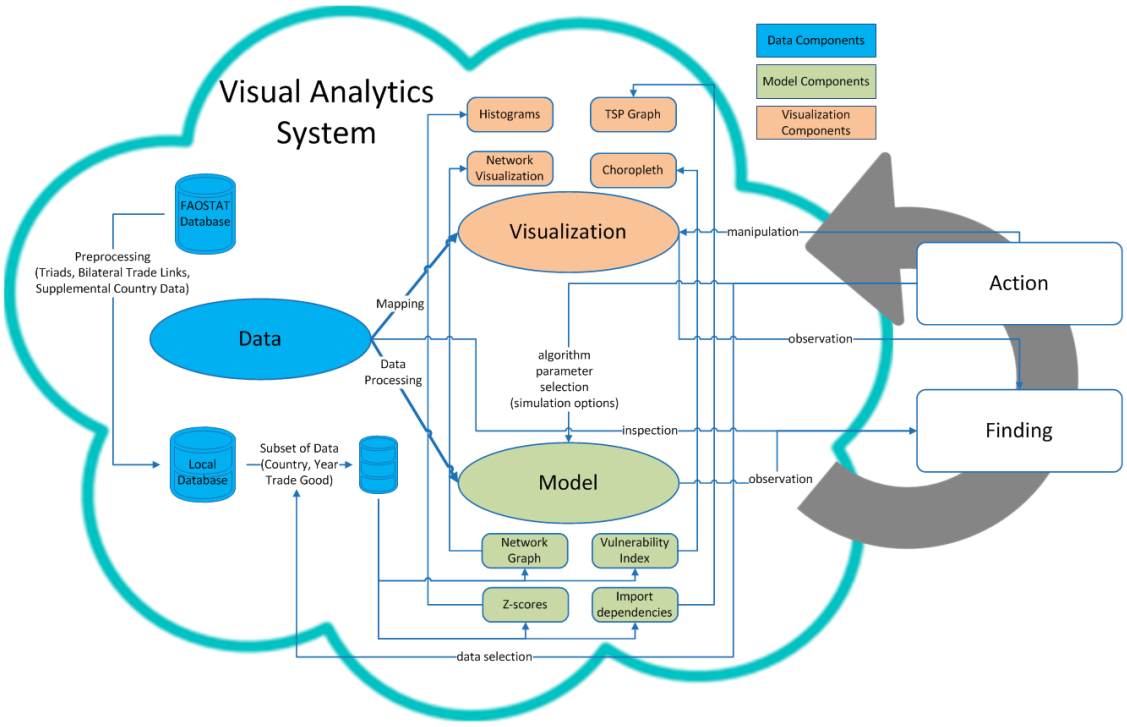

Figure 3.1: Visual Analytics System diagram, (motivated by Sacha *et al.* (2014))

links based on the import dependency for four staple crops, with the most opaque indicating the currently selected crop. Figure 3.2-2 shows the network graph, a visual representation of the food trade network, and all of the import and export trade links of the currently selected crop. Figure 3.2-3 is the choropleth map which visualizes the impacts of the simulated climate event from Figure 3.2-5. Both the network graph and choropleth map allow for a user to select a country for the simulation by clicking on the node in the graph or country on the map. The selected country is then given a dark border in both views as seen in Figures 3.5 and 3.8. Figure 3.2-4 shows the normal triad significance profile (TSP) graph based on four staple crops for the year 2013 overlayed with the TSP graph of the currently selected data subset. Figure 3.2-5 shows the parameters for the climate event simulation engine. In each of the sections moving the mouse over pertinent parts of the visualizations displays a tooltip for displaying detailed information, as in Figure 3.3. This tooltip displays the trade

link data from a link of the 2013 wheat network graph. In 2013 Egypt imported $576 million dollars which accounted for 23% of total Egyptian wheat imports and 11% of the total Egyptian imports of four staple crops.

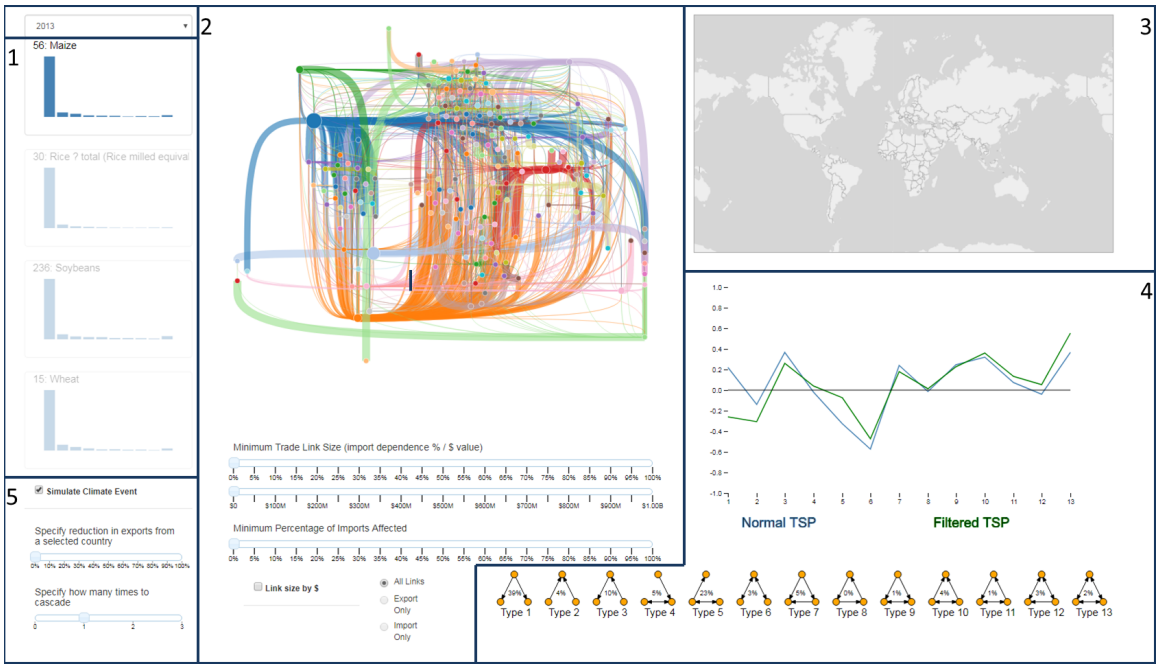

Figure 3.2: Sections of the dashboard. 1: Histograms of trade link import dependencies grouped by crop; 2: Network graph and filtering options; 3: A choropleth map visualizing the impacts of a simulated climate event; 4: Triad significance profile graph; 5: Climate event simulation engine parameters.

Figure 3.3: A tooltip is displayed when the user moves their mouse over pertinent parts of the visualizations. In this example a tooltip displays the trade link data from a link of the 2013 wheat network graph. The tooltip shows the trade link values for that year. In 2013 Egypt imported $576 million dollars which accounts for 23% of Egyptian wheat imports and 11% of the total Egyptian imports of four staple goods.

3.3.1 Simulation Option (Figure 3.2-5)

The simulation of climate events is the defining part of the system. This section allows for the parameters for the climate event simulation to be defined. The first checkbox in Figure 3.2-5 indicates whether we want the simulation engine to run or not. The calculations for the simulation engine are time consuming so generally this is only checked after an interesting scenario is identified. The other controls in Figure 3.2-5 only appear if the checkbox is checked and the choropleth map (Figure 3.2-4) will only be colored in if a simulation is being ran.

The slider in the next part of Figure 3.2-5 indicates the total percentage of reduction in export links to simulate. The last slider in Figure 3.2-5 indicates how many times the reduction should cascade down. Cascading zero times implies that only the selected country's direct importers are affected. Addition of the first cascade level will add the second-order effects of trade link disruption to the initial importer's export partners.

3.3.2 Histograms (Figures 3.2-1, 3.4)

The histogram charts in Figure 3.2-1 show the distribution of trade links, based on import dependency (Equation 3.2), for each of the four staple crops. The trade links are binned in increments of 10 percent. The first group is 0 to 10%, the next 10 to 20%, et cetera. The more opaque histogram chart indicates the currently selected good and clicking on any of the other histograms changes the selected good to the clicked chart. The y-axis of the histogram shows the quantity of trade links in each bin and the x-axis is the import dependency. For example, the furthest right bin represents the trade links which account for 90 to 100% of the importing country's entire import portfolio of the trade good. The tooltips (example in Figure 3.4) in

this section show the number of trade links in a bin and the top 10 trade links by dollar value. The trade link data shown on the tooltip is the exporting country, the importing country, the dollar value and the import dependency.

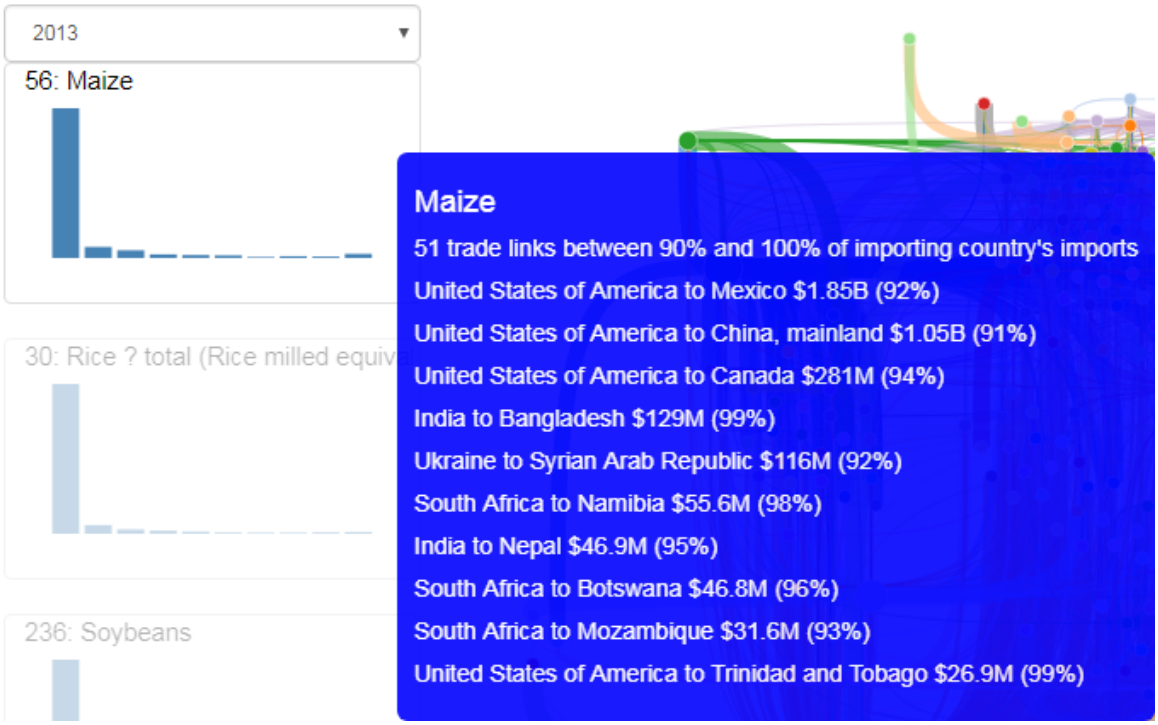

Figure 3.4: A zoomed in view of the histogram for corn in 2013, with the tooltip showing information for the last bin. The trade links are binned into groups based on their percentage contribution to the importing country's total imports of that product. This can be used to quickly identify countries who have a large dependency on a singular trade link. The tooltip here shows that, in 2013, Mexico's import of corn was almost exclusively (92%) from the United States at a trade value of $1.85 billion.

Generally, links in the left-most bins indicate more diversified imports and the right-most indicate imports that are made up of fewer trade links. This can be used to quickly identify countries that have a large dependency on a single trade link. As international food trade grows identification of reliance on imports is important to identification of vulnerability. Results from d'Amour *et al.* (2016) and Gephart *et al.* (2016) suggest that diversification of trade partners reduce food security risks.

An example is present in Figure 3.4. The presence of bins in the far right group

in the histograms for corn (Figure 3.4) indicate that there is a large dependency for some countries on a single trade link. Mousing over the last bin and displaying the tooltip (Figure 3.4, tooltip) shows that in 2013 Mexico relied on the United States for about 92% of its corn. Domain experts would be able to associate these types of links to potential areas of concern. If the importing country also exports we have the potential for the appreciation of cascading effects. By looking at bins that are in the at-risk group (furthest right in Figure 3.4) we can hover over the histogram and view the trade link information and corresponding import dependency. In this way the histograms can be used to select a country in the network graph or on the map as a starting point for exploration.

With a country selected (e.g. Mexico) analysts would be able explore further questions such as: if a climate event affected the United States in a manner that was significant enough to prompt the United States to stop shipping corn to Mexico, even temporarily, what cascading effects do we see? Are any countries dependent on imports from Mexico? We are able to visualize these first- and second-order effects in the network graph and choropleth map.

3.3.3 Network graph (Figure 3.5)

The international food trade market can naturally be represented by a weighted directed network graph as in Figure 3.5. Nodes of the graph are countries involved in trade and the edges are the trade links associated with the two countries. The node size is a function of the total GDP of the country. Node color is arbitrary but is constant for the life of the visualization. The nodes are positioned close to geographically correct with some perturbations for visual readability. Direction is indicated by color, the edge takes the color of the exporting country. For instance in figure 3.5 the United States is blue and all export links from the United States are

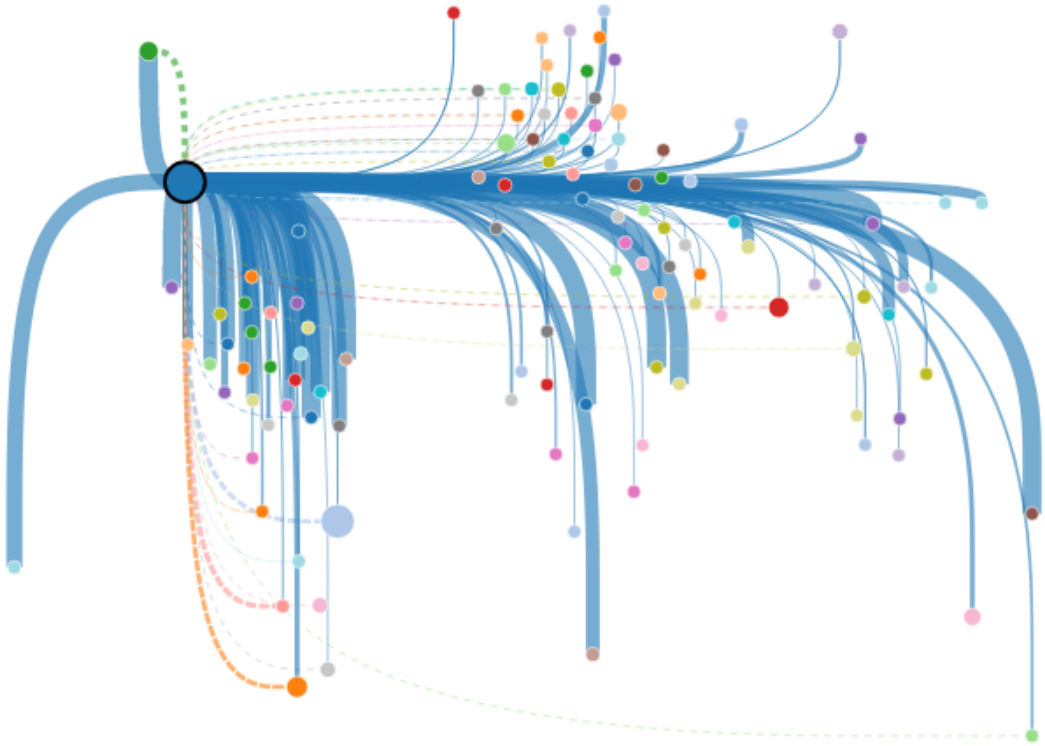

Figure 3.5: A network graph showing all the corn that was imported or exported to the United States in the year 2013. The selected country is indicated by the dark outline of the node, in this case the United States (large blue dot on the left side). Node size is a function of the total GDP of the country. Solid lines indicate export trade links from the selected country if applicable. Dashed lines indicated import trade links to the selected country. Depending on the option selected the thickness of the trade links indicate the trade link's contribution to the importing country's total staple good imports or the trade link's dollar value.

colored blue. Import links to the United States take the color of the exporting country, as. In the default view the weight of the link is the import dependency (Equation 3.2) of the trade link. The weight of the link is indicated by the thickness of the line representing the edge. There is also an option (Figure 3.6) to display the link size by dollar value. If no country is selected solid lines indicate both import and export trade links. If a country is selected its node will have a dark outline as in Figure 3.5. The large blue dot on the left side of the graph shows the selected country, in this case the United States. The edges are represented by solid lines, indicating export

trade links from the selected country, and dashed lines, indicating import trade links to the selected country. If a climate event is being simulated alternating dashes and spaces indicate a link broken by the export reduction of the simulation.

The three sliders in this section (Figure 3.6) filter the network graph. The first slider in Figure 3.6 hides any trade links that have an import dependency of less than the selected value. This is used to potentially filter out insignificant trade links, e.g. accounting for 1% of a country's total imports. The second slider filters out any trade links whose raw dollar value is not at least the selected value. Again this can be used to filter out insignificant links such as a trade link of $1,000 dollars. The third slider is only visible in simulation mode and is used to filter out nodes whose total imports are affected by at least the slider's current value. This is useful for determining which countries are significant affected, including cascading effects, by the simulated climate event. The single checkbox will show the links weighted by dollar value instead of the import dependency (Equation 3.2). The group of radio buttons will determine which type of links are shown. This is only available when a country is selected and not in simulation mode. There is also behavior for panning, zooming and node repositioning to facilitate interaction.

The network graph is used to visualize trade links in the international food trade network. As risk is a function of import dependency the thickness of the link indicates the importance of that trade link to the importing country. Selecting a country here will filter the data to only include exports from and imports to the selected country. It is also required for any climate simulation as we need to define the country who will have their exports reduced.

Continuing on the example from above, Mexico is the selected country and the trade links to and from Mexico are inspected. The tooltip for the link in the network graph (Figure 3.7, tooltip) shows that although the trade link provides approximately

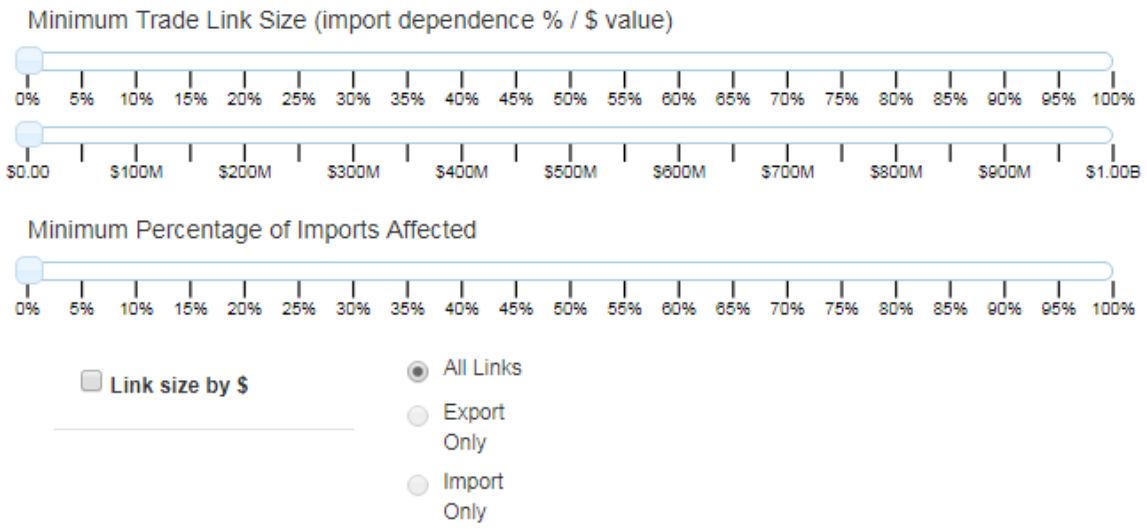

Figure 3.6: Options for filtering and display of the network graph. The first slider hides any export trade links that contribute less than the selected value to the link's importing country's total import value of the trade good. The second slider filters out any trade links whose raw dollar value is not at least the selected value. The third slider is only visible in simulation mode and is used to filter out nodes whose imports are affected by at least the slider's current value. The single checkbox will show the links weighted by dollar value instead of the import dependency (Equation 3.2). The group of radio buttons will determine which type of links are shown. This is only available when a country is selected and not in simulation mode.

92% of the corn imported to Mexico (from the histogram), it only accounts for about 37% of the total imports of staple goods. This percentage can be used by a domain-expert to gauge the diversity of imports across the staple goods of the importing country to further evaluate the level of vulnerability.

With a country selected analysts would also be able to see trade links upstream of a country. An example of this is in Figure 3.7-2. Mexico is the selected country (purple) and the network graph is showing corn trade links for 2013, with trade links filtered by import dependencies of 25% and dollar values of at least $250 million. This has the effect of showing only the more significant trade links to and from Mexico. The large dashed line, indicating an import trade link, into Mexico shows that Mexico is highly dependent on the United States for a large portion of its corn (92% from 3.7-1, tooltip). The solid line, indicating an export link, out of Mexico shows that

Venezuela is moderately dependent on Mexico for corn (29% from 3.7-2, tooltip). This would aid to identify countries that act as middle men, countries that also export the good they import. These countries' export partners are more susceptible to cascading effects due to climate events affecting their supply partner. This is especially true if the middle man has a high dependency on a single trade link as in this example of Mexico and the United States.

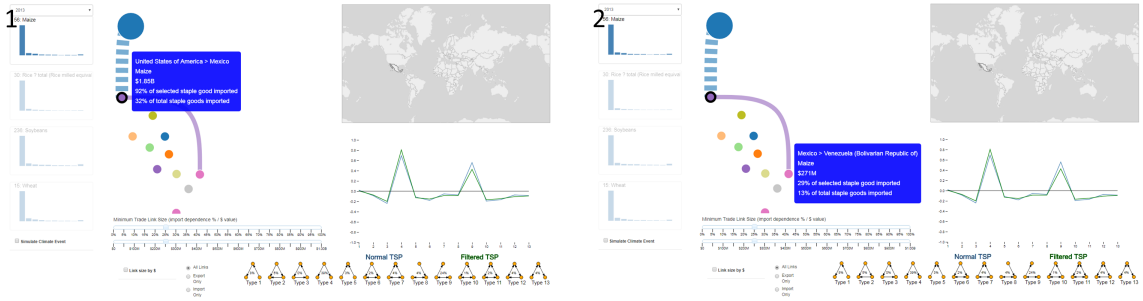

Figure 3.7: A network graph showing corn that is imported or exported to Mexico(purple). The United States is shown in blue and Venezuela is shown in pink. The network graph has Mexico as the selected country and is filtered to only include export trade links that account for greater than 25% of the link's importing country's total imports of the trade good. The large dashed line into Mexico shows that Mexico is highly dependent on the United States for a large portion of its corn (92% from 1, tooltip). The solid line into Venezuela shows that Venezuela is moderately dependent on Mexico for corn (29% from 2, tooltip).

3.3.4 Choropleth Map (Section 3, Figure 3.8)

The choropleth map in Figure 3.8 shows all countries. The choropleth map is always present, but only colored when a country is selected either here or in the network graph. The positioning in the network graph mirrors the topological layout here to aid in identification of countries without cluttering associated with labels. The choropleth map in Figure 3.8 gives a visual representation of the vulnerability index by affecting the intensity of coloring based on the loss of imports due to the simulated export reduction from the selected country as defined in Equation 3.1.

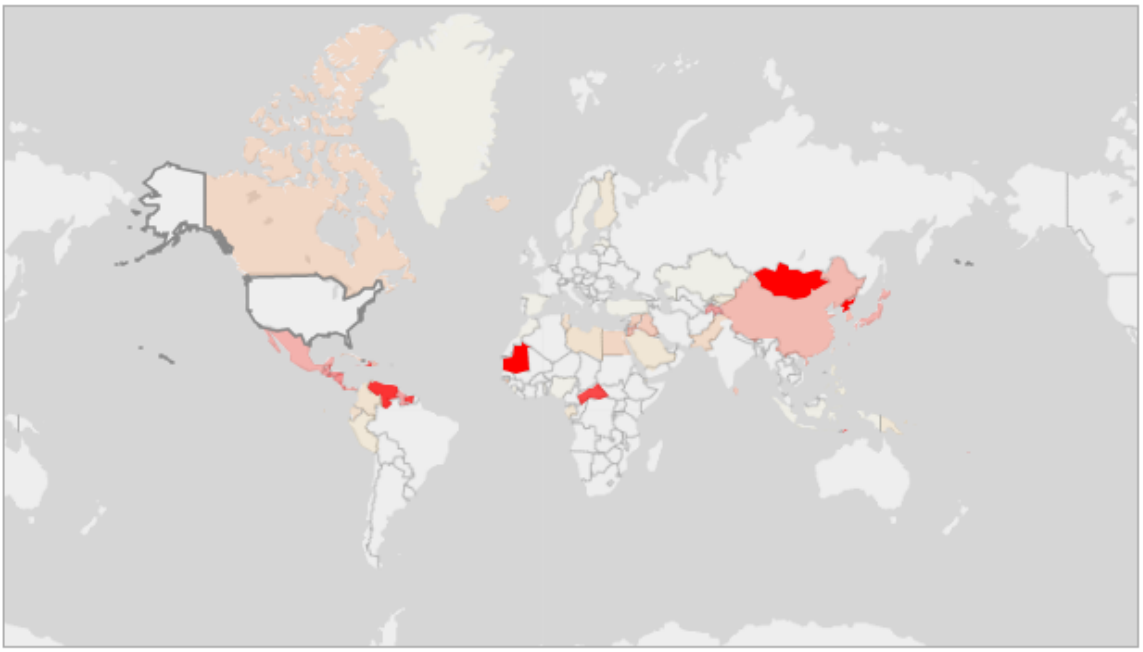

Figure 3.8: The choropleth map indicates the impact of a simulated climate event in the selected country on the downstream trade links. In this instance the United States experienced a climate event that reduced the value of corn exports by 10%. The darker and more red the country is colored, the greater the impact. In this simulation Canada, China, and some central African countries were the most impacted by the event.

Anything above 10% is red and the opacity increases beyond that. If the number of times to cascade is greater than zero, it is possible for the selected country to also be affected. The tooltips in this section show the total imports and exports of the selected good by the country. In the event of a simulation the affected import value, the affected import value to total import ratio, and the affected import value to total trade ratio (Equation 3.1) are also displayed.

The choropleth map is used for identification of vulnerable countries based on the climate event simulated. The more intense and more red the coloring, the higher the vulnerability.

An interesting example of this is Australia. Simulating a 25% reduction in 2013 wheat exports (Figure 3.9) results in the loss of nearly 95% of Australia's wheat

imports. This is because New Zealand loses $38 million in wheat trade from Australia and since New Zealand overall exports only $3 million all trade links are essentially removed in the simulation, including the trade link back to Australia. However, Australia is not colored in heavily in the choropleth map because the loss of the $600,000 trade link is not a significant percentage of the $5.79 billion total wheat trade Australia is involved in.

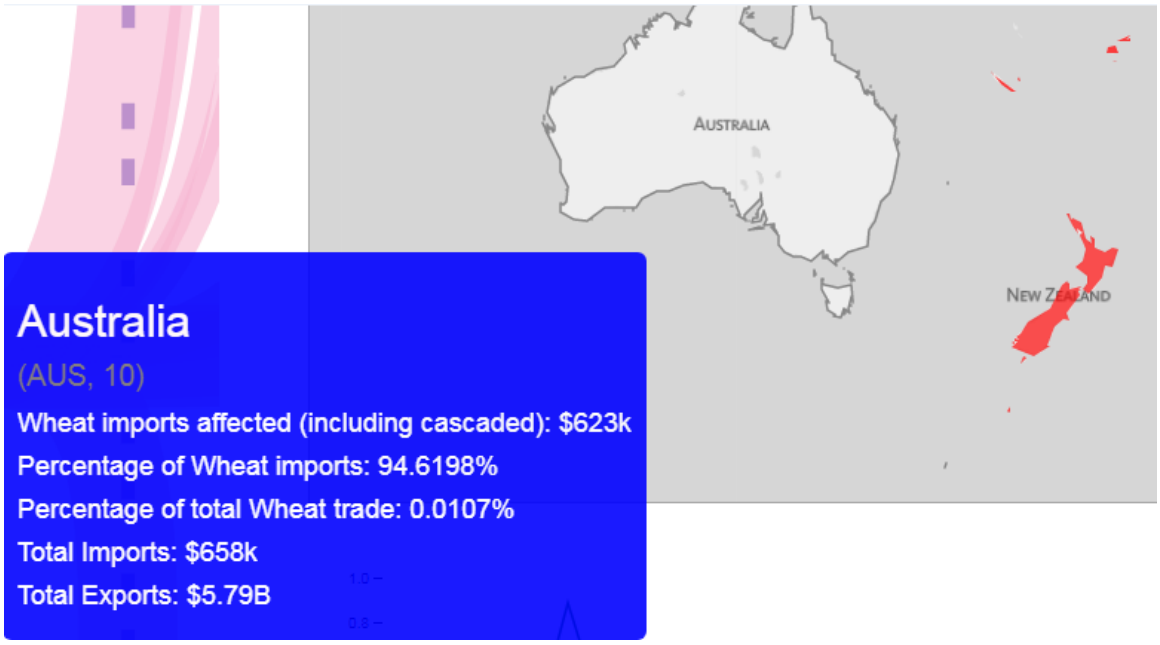

Figure 3.9: In this simulation Australia experienced a climate event that reduced the value of wheat exports by 25%. New Zealand is heavily affected and most of Australia's import links are broken. However, Australia is not colored in heavily in the choropleth map because the loss of the $600,000 trade link is not a significant percentage of the $5.79 billion total wheat trade Australia is involved in.

3.3.5 Triad Significance Profiles (Section 4, Figures 3.2-4, 3.11)

Figure 3.2-4 displays a normal triad significance profile (TSP) graph alongside the TSP graph for the current subset of data based on any filtering (e.g. selected country or minimum trade link size). In Figure 3.2-4 the x-axis in the graph indicates the triad configuration type as shown in Figure 3.10. Figure 3.10 shows the 13 different possible

configurations in a directed network graph. In Figure 3.10 the triad distributions for the network graph of corn in 2013 are also shown. These percentages change based on the current subset of data. The y-axis in Figure 3.2-4 shows the normalized z-scores defined as

$$z_i = \frac{N^{actual} - N^{random}}{stdev(N^{random})} \tag{3.3}$$

where N^{actual} is the actual number of triads of this type and N^{random} is the number of the same type in a randomly generated graph. A positive z-score indicates that the triads occurs more frequently than in a randomly generated network graph, and a negative value less frequently. The blue line shows the normal TSP for all 4 goods across all years of data and the green line is the TSP of the filtered data.

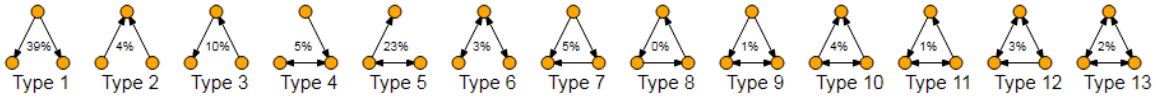

Figure 3.10: The 13 different triads. The percentages here are the distribution of triads for corn in 2013. These values will change with the filtering of data.

Triad significance profiles can aid in the classification and comparison of the network across different types of systems (Shutters and Muneepeerakul, 2012). Certain motifs are more or less present in the superfamily identified. Being able to visualize the TSP of the currently filtered data may assist in an assessment of the health of the filtered trade links. Overall, the research in this thesis focused more on cascading impacts to the trade network, but future work will explore the impact of removing network connectors on distributions of triads.

In the data for corn there are some interesting findings. In 1988 (Figure 3.11, left) we see one dominating triad, type one, which appears a lot more frequently than a random graph would suggest. Note that this triad does not include any bilateral trade links. Progressing from 1988 to 2013, we see the z-score of type nine, ten and thirteen, which all contain bilateral trade links, increase significantly (Figure 3.10,

right) and a decrease of type one and two, both unilateral triads. This may indicate an increasingly connected trade network. The increase of type three triads, in which the connecting node acts as a middle man, may suggest the possibility of cascading effects is increased.

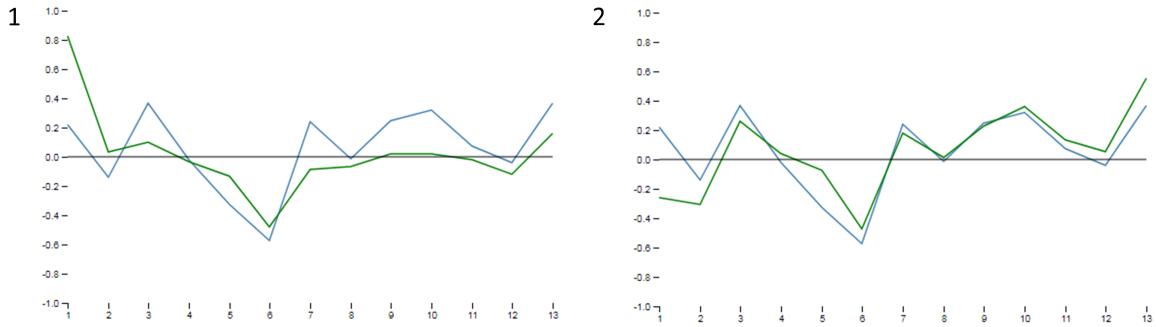

Figure 3.11: The is a graph that overlays the current triadic significance profile (TSP) with the normal TSP. The graph on the left is the 1988 wheat TSP and the graph on the right is 2013 wheat TSP.

3.4 Enhancement Over Existing Visualizations

An emphasis of this visual analytics system is the consideration of the global trade network in its entirety. Neither of the reviewed visualizations take into consideration the topology of the food trade network. The FAOSTAT visualization represents only a single point in the food trade network. This does not allow for a direct interpretation of cascading effects. My tool visualizes the entire global trade network. The visualization offered by the Met Office 2.1 shows an index of food insecurity at a global scale. The focus is on overall vulnerability to food insecurity and does not visualize direct responses to climate events. The interaction and simulated climate events offered by my visual analytic system allow for the exploration of second-order effects of climate events by direct visualization of the affected trade links in the network graph and coloring in the choropleth map.

Chapter 4

CASE STUDIES

In this section two case studies are examined. The first is the 2011 Chinese drought and the second is a simulated future event where the United States corn exports are reduced. The first case study shows the basic use of the system and shows how we can identify vulnerable countries based on simulated climate events. Although the first case study does not highlight the cascading effects it does show that the vulnerability of a country may be affected by the simulation of a climate event. In our second case study we explore a full use case scenario of the system by targeting one of the largest corn exporters, the United States, and simulating a moderate climate event. In doing so we highlight the cascading effects to the food trade network and visualize the potentially vulnerable countries affected by a simulated climate event.

4.1 2011 Chinese Drought

In 2011 the United Nations food agency issued an alert warning that a severe drought was threatening the wheat crop in China, the world's largest wheat producer, and resulting in shortages of drinking water for people and livestock (Bradsher, 2011). In response to the drought China was forced to import more wheat instead of relying on its self sufficiency as in previous years (Sternberg, 2012). The increase in demand drives the price of wheat up as show in Table 4.1. This coupled with a number of countries implementing export bans the previous year (Fellmann *et al.*, 2014) has a great potential for a disrupted food trade network.

Country	Market Year	Wheat Price USD / Ton	Exported to China (million USD)
Australia	2010	$200.00	$179
Australia	2011	$265.10	$180
Australia	2012	$235.00	$628
Australia	2013	$302.20	$242
Canada	2010	$177.10	$72
Canada	2011	$237.00	$63
Canada	2012	$253.90	$163
Canada	2013	$252.90	$300
USA	2010	$209.00	$36
USA	2011	$266.00	$159
USA	2012	$286.00	$224
USA	2013	$252.00	$1,292

Table 4.1: Wheat price data for years 2010 - 2013 (FAOSTAT Producer Prices - Annual) (FAO, 2016)

Halfway around the world in Egypt, the world's largest importer of wheat, was the resonance felt; wheat prices doubled the price of bread tripled (Sternberg, 2012). According to Croppenstedt *et al.* (2006) bread provides around one-third of the daily Egyptian caloric intake. These two factors prompted bread shortages and price increases in parts of the country that contributed to bread-inspired demonstrations and directly influenced political protest.

During this time many export restrictions were in place, including Russia's export ban (Fellmann *et al.*, 2014). For simulation purposes, we model this export ban a 100% export reduction out of Russia and run the simulation to see the vulnerable countries. Modeling it in this way allows us to see a number of countries significantly

affected by the ban. Among them is Egypt, as anticipated, displaying an almost 40% loss of imports (Figure 4.1, tooltip). From the red coloring in the choropleth map (Figure 4.1), the visual analytic system marks this as a potential area of vulnerability. Examining the network graph by filtering for very large links (great than $500 million), Figure 4.2-1 shows Egyptian imports of wheat from their main providers. In 2011 Egypt imports over $2 billion from the United States and Russia. In 2013 that number is reduced to just $1.1 billion. Though I make no claims of correlation, the 40% reduction postulated from the simulation mirrors what is seen in Figure 4.2.

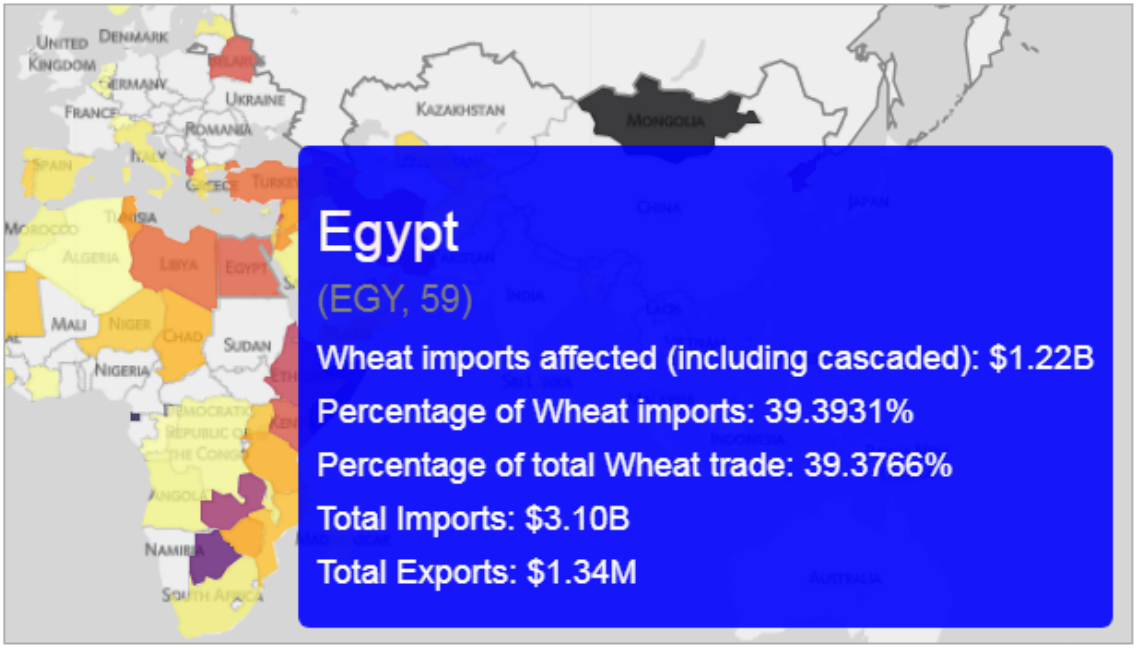

Figure 4.1: Choropleth map of simulated Russian wheat export ban. The red color indicates that Egypt is moderately vulnerable to a climate event forcing an export reduction from Russia. The tooltip shows that Egypt would lose about $1.22 billion in wheat imports accounting for almost 40% of their entire import of wheat.

Another aspect of analyzing the 2011 Chinese drought is supported by the system is exploration of the temporal changes to the food trade network by visualizing the graph year over year, as in Figure 4.3, to look for patterns. We expect that there will be changes to the food trade network because of the aforementioned 2011 Chinese

drought. The views in Figure 4.3 are set by selecting the first year to examine, 2010, and then filtered the network graph to only show links of greater than $50 million. Each successive view only the year was modified.

As expected, looking at the graph we notice this sharp increase in imports of wheat to China. In 2010 China is largely self-sufficient; with imports of only $296 million (Figure 4.3-1, tooltip). In 2011 and 2012 we see still more increases in imports. Finally, moving to 2013, Chinese imports of wheat increased to $1.90 billion (Figure 4.3-4, tooltip), an increase of 640%. The links go from virtually non-existent (figure 4.3-1 US to China, $56M in 2010, link not visible) to a trade link that is of a significant value (Figure 4.3, bottom left; US to China, $1.292 billion in 2013, large blue line). Moreover, from this progression we see the shift from Chinese self-sufficiency to import dependency.

From this case study we have demonstrated that our visual analytic system can help analysts explore the impacts of historical climate events on the international food trade network.

Figure 4.2: Left: In 2011 Egypt (light blue) imports $852 million in wheat from the United States (dark blue) and $1.219 billion from Russia (pink). A total of approximately $2.071 billion; Right: In 2013 Egypt (light blue) imports $558 million in wheat from the United States (dark blue) and $576 million from Russia (pink). A total of approximately $1.134 billion is close to half of the value imported just two years ago.

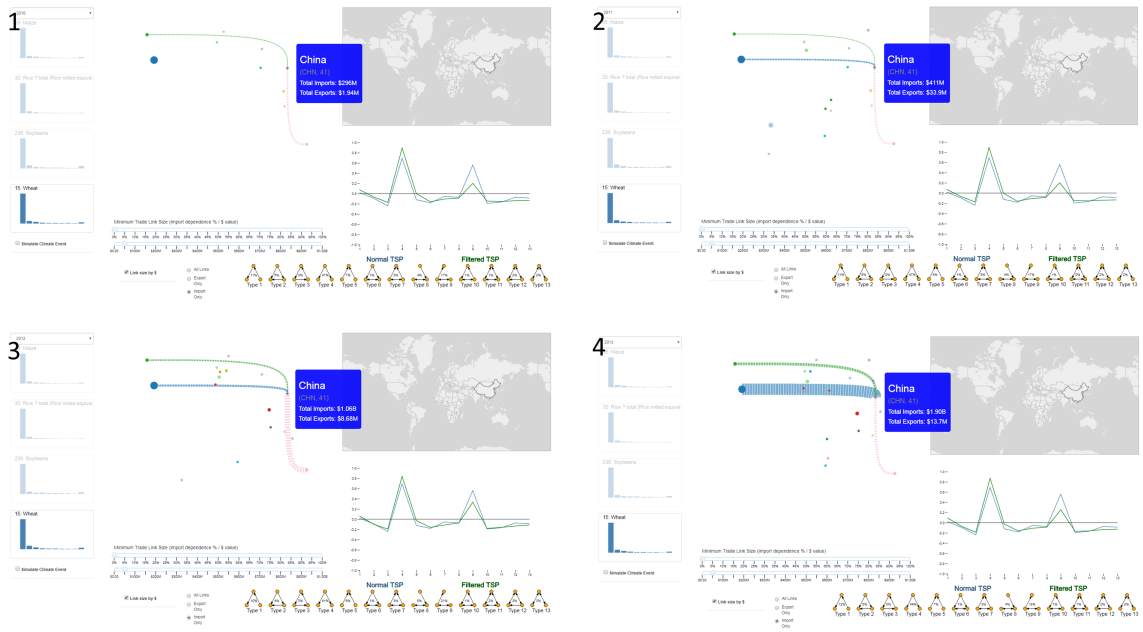

Figure 4.3: Progression of significant Chinese wheat imports from 2010 to 2013. Top Left: In 2010 China (purple) imported $36 million in wheat from the United States (blue, link not shown), $72 million from Canada (green) and $179 million from Australia (pink). From the tooltip China imported a total $296 million; Top Right: In 2011, during the first year of the crisis, China (purple) imported $159 million in wheat from the United States (blue), $63 million from Canada (green) and $180 million from Australia (pink). From the tooltip China imported a total $411 million; Bottom Left: By 2012, with a sharp increase in imports directly related to the drought, China (purple) imported $224 million in wheat from the United States (blue), $163 million from Canada (green) and $628 million from Australia (pink). From the tooltip China imported a total $1.06 billion, almost four times the amount in 2010.; Bottom Right: By 2013 China (purple) being increasingly dependent on the $1.292 billion imported from the United States (blue), $300 million from Canada (green) and $242 million from Australia (pink). From the tooltip China imported a total $1.90 billion, a more than six-fold increase from 2010.

4.2 Simulated 2020 US Climate Event

As a second case study, we will use the system to simulate the effect of an unspecified climate event to the United States. As a demonstration we will highlight the downstream effects of a major reduction in exports of corn from the United States.

Although the United States was chosen a priori, we could have used the 2013 trade data as a starting point to start the selection process for a country. This can be done by first inspecting the histograms. The tooltip in Figure 4.4 shows three major importers, in both dollar value and import dependency, of United States' exports of corn: Mexico at $1.85 billion and 92%, China at $1.05 billion and 91% and Canada at $281 million and 94%. However, as import dependency is a function of the export value as well (Equation 3.1) we confirm import dependency on the network graph. To do so we filter the network graph to show only countries with an import dependence of at least 75% and trade link values of at least $100 million (Figure 4.4, sliders). Note that in this instance we could have filtered the network graph first, but using the histograms allows for the inspection of smaller countries. We do see two of the identified links still present (Figure 4.4, the two blue lines) with this filtering (the United States to Mexico and the United States to China) and so we decide to continue the analysis with the United States as the selected country. As the United States is one of the major exporters of corn ($6.98 billion in 2013 according to the tooltip in Figure 4.5-1), we expect to see a number of vulnerable countries, even ones with no direct trade links with the United States. A 15% export reduction is chosen arbitrarily as a starting point.

As the United States was chosen as a potential candidate for simulation, we select the node representing the United States (large blue node, approximately geographically positioned). The node and country in the map are drawn with dark borders

Figure 4.4: The process of selecting a country for the simulation starts with looking at the histograms and confirming on the network graph. Here the tooltip for the histogram displays the name of exporting and importing country along with the dollar value and import dependence of the trade link. This shows multiple potentially import dependent countries as indicated by a high import dependence percentage. The dependencies can be confirmed with filtering on the network graph (sliders on the bottom). The links remaining visible (the United States to Mexico, the United States to China, India to Bangladesh and Ukraine to the Syria Arab Republic) coincide with the histogram information.

to indicate it has been selected (Figure 4.5-1). As expected, and as shown in the network graph (Figure 4.5-1), there are a large number of countries involved in corn trade with the United States. Next the *Simulate Climate Event* checkbox is selected and we select a 15% reduction as shown in bottom left of Figure 4.5-2. The network graph in Figure 4.5-2 shows there are a large number of cascaded effects, represented by the now visible trade links. However, further filtering is required to gain con-

text. In Figure 4.5-3 the *Minimum Percentage of Imports Affected* is changed to 30%. This filters the network graph to only display the links affecting those countries whose imports have been reduced by at least 30%. Examining the choropleth map of the current state in Figure 4.6, we see that Venezuela, North Korea and Mongolia are affected heavily based on the darker coloring.

To examine the impact on Venezuela we look at the trade links coming into Venezuela. The link from the United States shows a reduction of only $55.5 million (Figure 4.5-4, tooltip), which is significantly less than the $301 million shown in the country's information (Figure 4.7-1, tooltip). To look for other major import sources we slowly adjust the trade link size by dollar filter until only the top few links are shown (Figure 4.7-2, second slider has moved to $200 million). Examining the link from Argentina to Venezuela (Figure 4.7-2, tooltip) shows a loss of only $41k which has relatively little impact to the $301 million loss. Examining the other link, Mexico to Venezuela, reveals the cascaded effect. Figure 4.7-4, tooltip, shows that Mexico's trade link to Venezuela has been reduced by $240 million, a significant portion of the $301 million total import loss to Venezuela. The export reduction of 15% from the United States prompts a loss of $280 million to Mexico (Figure 4.7-4) which is mostly passed on to Venezuela. Thus, Venezuela is indirectly impacted by a climate event to the United States, to the degree of approximately one third of their entire import of corn.

Another example of use would be to see countries that are significantly (e.g. import losses of greater than 75%) impacted by the climate event. We adjust the *Minimum Percentage of Imports Affected* to 75% (Figure 4.8-1) and *Minimum Trade Link Size* to $25 million to filter out the insignificant trade links. As indicated by the dark coloring in the choropleth map in Figure 4.6, the impact to North Korea is significant. However, no solid blue line (export from the United States) connects to North Korea

(brown dot) in Figure 4.8-1 so no direct link exists from the United States to North Korea. Yet North Korea's imports are simulated to be affected by almost 80% (Figure 4.8-2, tooltip). By examination of the link (Figure 4.8-3) we conclude that China acts as a middle man. The tooltip in Figure 4.8-4 shows that China lost imports of $158 million. The same tooltip shows that it only exports $34.2 million. Since the loss of imports is assumed to be first mitigated by reduction of exports, China essential breaks all export links to recoup the $158 million loss of imports. This is a potential limitation of the system as China may still export the relatively small amount of $31.9 million (Figure 4.8-3) to North Korea depending on a number of factors. (e.g. political repercussions, temporal considerations such as season). This example shows the cascading effect of the loss of imports to China from the United States being propagated to North Korea.

This case study highlights the usefulness of these cascading, second-order effects. In the example of Venezuela we are able to see that Venezuela is more heavily affected than the direct trade link would suggest. In the example of North Korea there is no direct trade link and without cascading effects being accounted for, the vulnerability to North Korea may not be considered at all. The ability to visualize these links facilitates the identification of these potentially vulnerable, import reliant countries. This is even more apparent when those countries are dependent on a small number of suppliers as seen in both cases presented here.

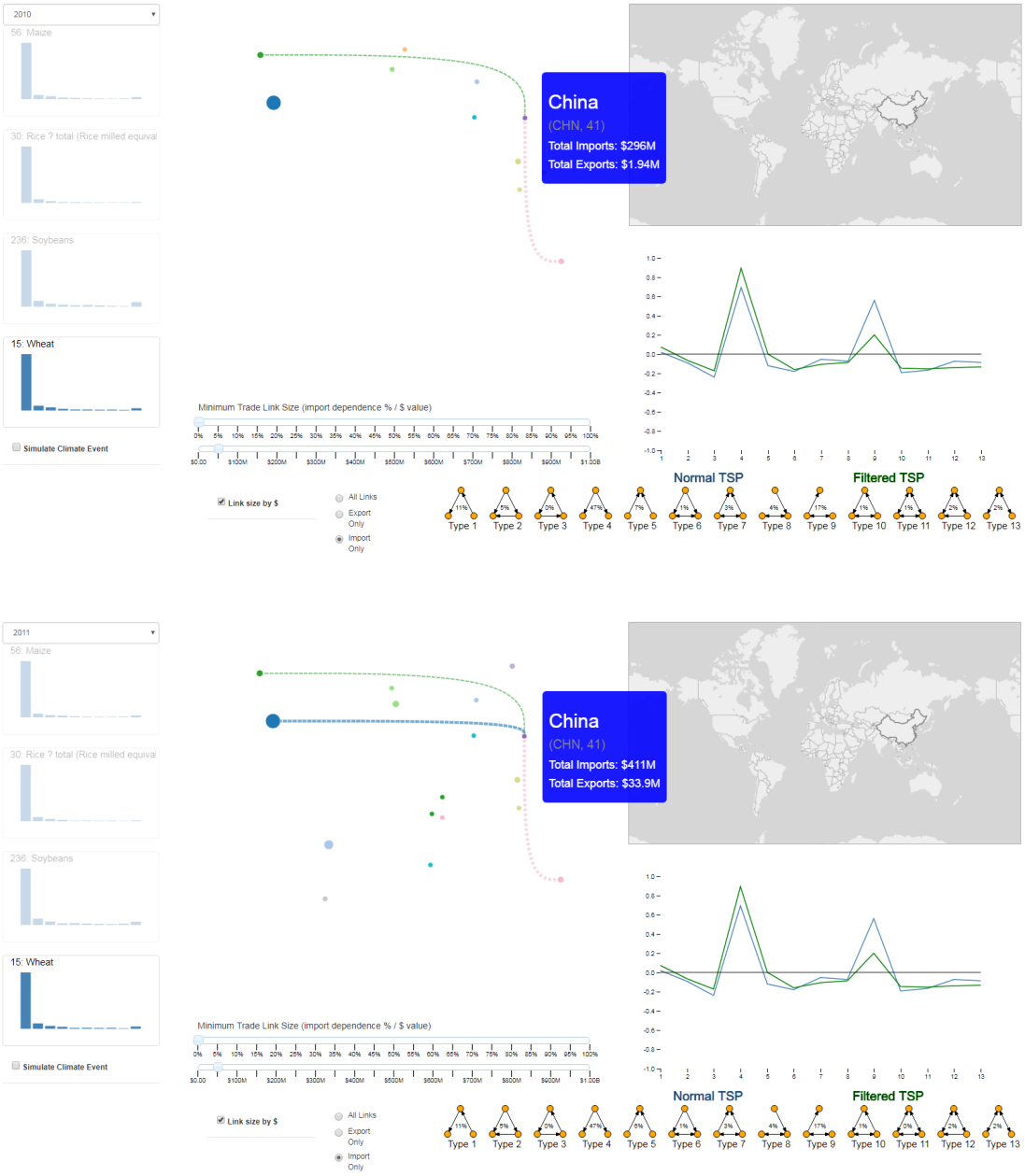

Figure 4.5: Running a simulation and exploring results. 1: The United States is selected; 2: Simulation is ran with a 15% export reduction from the United States; 3: Simulation results filtered on countries with import losses of at least 30% and showing only links of at least a $200 million dollar value; 4: Tooltip of the trade link from the United States to Venezuela

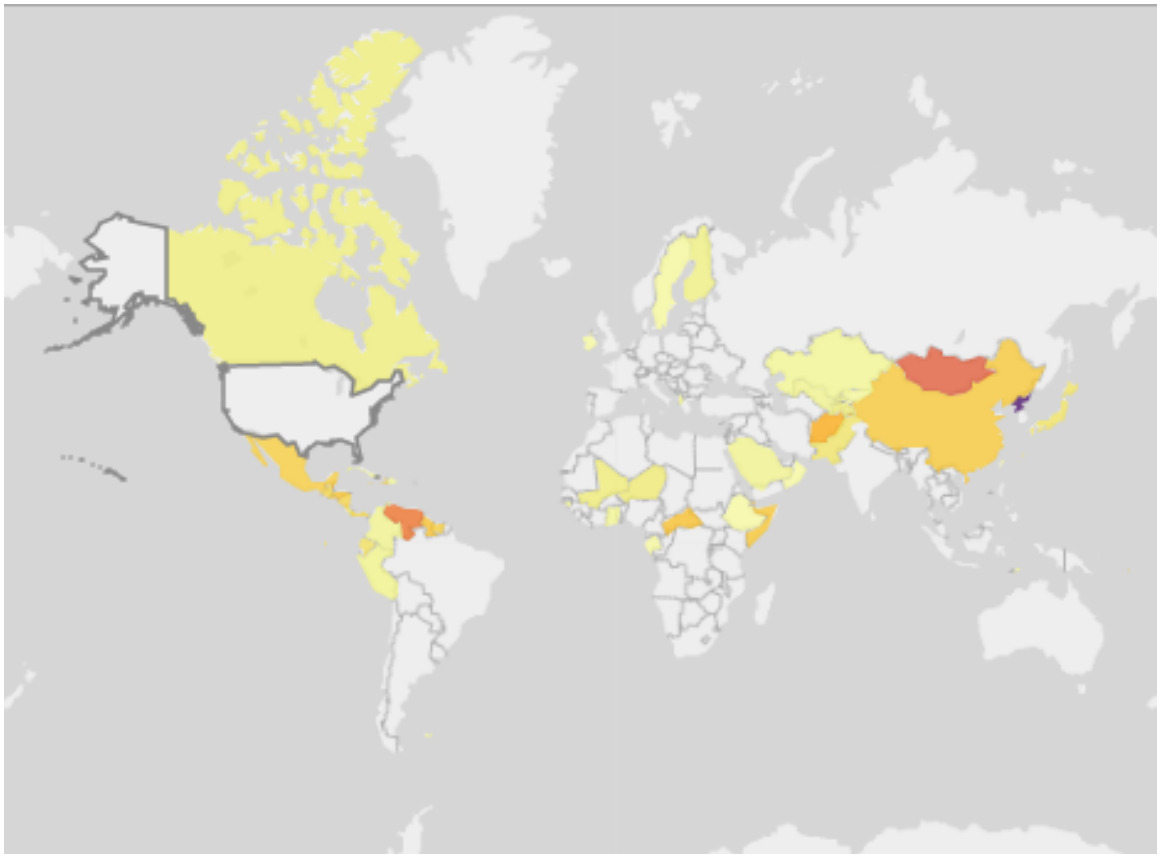

Figure 4.6: A zoomed in view of the choropleth map from the simulation.

Figure 4.7: Examining the results of a simulation, filtered on large dollar value ($200 million) and moderate import losses (30% loss). 1: Tooltip showing the impact to Venezuela; 2: Tooltip of the trade link from Argentina to Venezuela; 3: Tooltip of the trade link from Mexico to Venezuela; 4: Tooltip showing the impact to Mexico

Figure 4.8: Examining the results of a simulation, filtered on moderate dollar value ($25 million) and large import losses (75% loss). 1: Simulation results filtered on countries with import losses of at least 75% and showing only links of at least a $25 million dollar value; 2: Tooltip showing the impact to North Korea. The link is also drawn with alternating dashes and spaces, indicating it has been broken.; 3: Tooltip of the trade link from China to North Korea; 4: Tooltip showing the impact to China

Chapter 5

CONCLUSIONS

5.1 Summary

The goal of this thesis was to allow for effective visualization of the international food trade network, identification of potentially vulnerable countries and aid in prediction of level of food insecurity risk based on impacts of future climate variability. To achieve this goal a visual analytics framework was created for visual analysis and exploration of the network. This framework allows the domain expert to filter and manipulate the dataset. It also allows for a level of prediction by simulating the effect of a climate event. The framework helps determine downstream effects of a reduction in one country's exports beyond the first level of trade.

5.2 Limitations

The simulations on the dashboard are limited in scope to a single country and single staple good. In the case study of the 2011 Chinese drought this was an apparent limitation. It is known that there were a number of countries implementing export bans (Fellmann *et al.*, 2014) based on the climate event and being able to model all in one simulation would draw a better representation of the state of the global food trade network at the time. This would facilitate more accurate vulnerability modeling. Disallowing multiple crop types also is a limitation. Being able to work with all four of the staple goods at one would allow for exploration of gap coverages in staple crop imports. It would also allow a truer picture of the effect to food security to a country based on the simulated climate event.

There are also a number of limitations encompassed on the graphical user interface of dashboard. The majority of the computation of downstream effects is done on the front-end. This makes processing of the cascading links CPU intensive and anything beyond two iterations the dashboard becomes unresponsive. Holding such a large number of links in memory client side forces the inspection of a singular trade good at one time. Creation of such a large number of network graphs links as DOM elements allows for the interactivity of the dashboard but rendering on a HTML5 canvas would perform much better. This is also a limiting factor in the scalability of the network graph representation. Only the display of the four staple crops were chosen for this reason.

5.3 Future Work

There is a lot of potential for future enhancements. Addressing the above limitations would be the primary focus. The ability to add intelligence to weight trade links based on some criteria to allow for unequal distribution of remaining trade goods as a result of a climate event is another. This could potentially be achieved by geographical proximity or known relationship statuses between countries. In the choropleth, the visualization could also take into account other traditional vulnerability indices to affect the intensity of coloring.

Another avenue of future work would be to further explore network triad distributions and triad significance profiles (TSP) related to the international food trade network. For instance, how do changes to the international food trade network based on simulated climate events alter the distributions? Are the TSP affected as well and is there a change in motifs? Are there any patterns related to vulnerability and entrance to or exit from motif positions based on altered trade links?

Another potential improvement would be to affect the production of food goods

instead of just export link value. Food production could be limited to a point where there is actually a greater reduction in exports that the static loss of production. An example of this would be Russia's recent ban on exports of wheat during the 2011 drought to stabilize internal stores. FAOSTAT also has the production data in their database and being able to incorporate this data, along with population statistics, could prove very useful.

Another option would be improvement of the algorithm for the distribution of the remaining exports. It may not be realistic to assume that the country experiencing the export reduction would perfectly distribute the remaining exports among their trade partners. In reality the distribution of exports may be skewed towards the most proximal country or, more likely, the country willing to pay the most.

Another significant enhancement would be able to enhance the algorithm to associate water dependency of crops more accurately. Virtual water, the amount of water embedded in a particular good, is a current area of research and the system could be adapted to consider the virtual water as in the current well-defined models (Hoekstra and Hung, 2005). Alternatively if one crop is more dependent on water there could be a coefficient of impact to take that into account. Other research, such as Konar *et al.* (2011), has sought to explore the food trade in relation to the virtual water value of the commodity. Future research may make this conversion to account for not only reduction but possible increases in crop production.

The system could also be improved to take into account the temporal aspects of crop production. For instance, is the same good being traded between counties because of different growing seasons? Is a country more import dependent on different countries based on the time of year? There is potential to model the simulation based on the production of a crop, the season, and the geographical location.

As mentioned in the introduction, the scope of this system is not limited to climate

events or food trade. The system could be expanded to allow for trade of other goods, such as raw materials. This is particularly true if we are able to map a raw material to a production good. As an example, in the event of a reduction in silicon imports to a country, how could we model the reduction in computer chips, made with silicon, exports from that country? This is another cascading effect that may benefit from analysis.

REFERENCES

Andrienko, G., N. Andrienko, D. Keim, A. M. MacEachren and S. Wrobel, "Challenging problems of geospatial visual analytics", Journal of Visual Languages & Computing **22**, 4, 251–256 (2011).

Bostok, M. (Data Driven Documents, 2016), D3. JavaScript library d3js.org. Accessed 28 August 2017.

Bradsher, K., "Un food agency issues warning on china drought", The New York Times **8**, 2, 2011 (2011).

Brobakk, J. T. and R. Almås, "Increasing food and energy prices in 2008: What were the causes and who was to blame?", (2011).

Cook, K. A. and J. J. Thomas, "Illuminating the path: The research and development agenda for visual analytics", (2005).

Croppenstedt, A., M. Saade and G. Siam, "Food security and wheat policy in egypt", Roles of agriculture policy brief (2006).

d'Amour, C. B., L. Wenz, M. Kalkuhl, J. C. Steckel and F. Creutzig, "Teleconnected food supply shocks", Environmental Research Letters **11**, 3, 035007 (2016).

D'Odorico, P., J. A. Carr, F. Laio, L. Ridolfi and S. Vandoni, "Feeding humanity through global food trade", Earth's Future **2**, 9, 458–469 (2014).

Dunne, C. and B. Shneiderman, "Motif simplification: improving network visualization readability with fan, connector, and clique glyphs", in "Proceedings of the SIGCHI Conference on Human Factors in Computing Systems", pp. 3247–3256 (ACM, 2013).

Eades, P., W. Lai, K. Misue and K. Sugiyama, "Preserving the mental map of a diagram", Tech. rep., Technical Report IIAS-RR-91-16E, Fujitsu Laboratories (1991).

Fader, M., D. Gerten, M. Krause, W. Lucht and W. Cramer, "Spatial decoupling of agricultural production and consumption: quantifying dependences of countries on food imports due to domestic land and water constraints", Environmental Research Letters **8**, 1, 014046 (2013).

Fagiolo, G., J. Reyes and S. Schiavo, "The evolution of the world trade web: a weighted-network analysis", Journal of Evolutionary Economics **20**, 4, 479–514 (2010).

FAO (Food and Agriculture Organization of the United Nations, 2016), FAOSTAT. Online database fao.org/faostat. Accessed 28 August 2017.

Fellmann, T., S. Hélaine and O. Nekhay, "Harvest failures, temporary export restrictions and global food security: the example of limited grain exports from Russia, Ukraine and Kazakhstan", Food Security **6**, 5, 727–742 (2014).

Garlaschelli, D. and M. I. Loffredo, "Structure and evolution of the world trade network", Physica A: Statistical Mechanics and its Applications **355**, 1, 138–144 (2005).

Gephart, J. A., E. Rovenskaya, U. Dieckmann, M. L. Pace and Å. Brännström, "Vulnerability to shocks in the global seafood trade network", Environmental Research Letters **11**, 3, 035008 (2016).

Ghoniem, M., J.-D. Fekete and P. Castagliola, "A comparison of the readability of graphs using node-link and matrix-based representations", in "Information Visualization, 2004. INFOVIS 2004. IEEE Symposium on", pp. 17–24 (Ieee, 2004).

Godfray, H. C. J., J. R. Beddington, I. R. Crute, L. Haddad, D. Lawrence, J. F. Muir, J. Pretty, S. Robinson, S. M. Thomas and C. Toulmin, "Food security: the challenge of feeding 9 billion people", science **327**, 5967, 812–818 (2010).

Grochow, J. A. and M. Kellis, "Network motif discovery using subgraph enumeration and symmetry-breaking", in "RECOMB", vol. 4453, pp. 92–106 (Springer, 2007).

Hadley Center (Met Office, 2017), website www.metoffice.gov.uk/food-insecurity-index. Accessed 28 August 2017.

Headey, D., "Rethinking the global food crisis: The role of trade shocks", Food Policy **36**, 2, 136–146 (2011).

Herman, I., G. Melançon and M. S. Marshall, "Graph visualization and navigation in information visualization: A survey", IEEE Transactions on visualization and computer graphics **6**, 1, 24–43 (2000).

Hoekstra, A. Y. and P. Q. Hung, "Globalisation of water resources: international virtual water flows in relation to crop trade", Global environmental change **15**, 1, 45–56 (2005).

Hoekstra, A. Y. and M. M. Mekonnen, "The water footprint of humanity", Proceedings of the national academy of sciences **109**, 9, 3232–3237 (2012).

Holten, D. and J. J. Van Wijk, "Force-directed edge bundling for graph visualization", in "Computer graphics forum", vol. 28, pp. 983–990 (Wiley Online Library, 2009).

Hund, M., D. Böhm, W. Sturm, M. Sedlmair, T. Schreck, T. Ullrich, D. A. Keim, L. Majnaric and A. Holzinger, "Visual analytics for concept exploration in subspaces of patient groups", Brain informatics **3**, 4, 233–247 (2016).

Johnstone, S. and J. Mazo, "Global warming and the arab spring", Survival **53**, 2, 11–17 (2011).

Kali, R. and J. Reyes, "The architecture of globalization: a network approach to international economic integration", Journal of International Business Studies **38**, 4, 595–620 (2007).

Keim, D., G. Andrienko, J.-D. Fekete, C. Gorg, J. Kohlhammer and G. Melançon, "Visual analytics: Definition, process, and challenges", Lecture notes in computer science **4950**, 154–176 (2008).

Keim, D., J. Kohlhammer, M. Pohl, G. Santucci and G. Andrienko, "Solving problems with visual analytics", Procedia Computer Science **7**, 117–120 (2011).

Keim, D. A., F. Mansmann, J. Schneidewind and H. Ziegler, "Challenges in visual data analysis", in "Information Visualization, 2006. IV 2006. Tenth International Conference on", pp. 9–16 (IEEE, 2006).

Konar, M., C. Dalin, S. Suweis, N. Hanasaki, A. Rinaldo and I. Rodriguez-Iturbe, "Water for food: The global virtual water trade network", Water Resources Research **47**, 5 (2011).

Li, L., D. Alderson, J. C. Doyle and W. Willinger, "Towards a theory of scale-free graphs: Definition, properties, and implications", Internet Mathematics **2**, 4, 431–523 (2005).

MacDonald, G. K., K. A. Brauman, S. Sun, K. M. Carlson, E. S. Cassidy, J. S. Gerber and P. C. West, "Rethinking agricultural trade relationships in an era of globalization", BioScience **65**, 3, 275–289 (2015).

Milo, R., S. Shen-Orr, S. Itzkovitz, N. Kashtan, D. Chklovskii and U. Alon, "Network motifs: simple building blocks of complex networks", Science **298**, 5594, 824–827 (2002).

Porkka, M., M. Kummu, S. Siebert and O. Varis, "From food insufficiency towards trade dependency: a historical analysis of global food availability", PloS one **8**, 12, e82714 (2013).

Purchase, H., "Which aesthetic has the greatest effect on human understanding?", in "International Symposium on Graph Drawing", pp. 248–261 (Springer, 1997).

Ravasz, E. and A.-L. Barabási, "Hierarchical organization in complex networks", Physical Review E **67**, 2, 026112 (2003).

Rodgers, P., "Graph drawing techniques for geographic visualization", Exploring geovisualization pp. 143–158 (2005).

Sacha, D., A. Stoffel, F. Stoffel, B. C. Kwon, G. Ellis and D. A. Keim, "Knowledge generation model for visual analytics", IEEE transactions on visualization and computer graphics **20**, 12, 1604–1613 (2014).

Schiavo, S., J. Reyes and G. Fagiolo, "International trade and financial integration: a weighted network analysis", Quantitative Finance **10**, 4, 389–399 (2010).

Schmidhuber, J. and F. N. Tubiello, "Global food security under climate change", Proceedings of the National Academy of Sciences **104**, 50, 19703–19708 (2007).

Schnepf, R. D. and R. M. Chite, "Us agriculture after hurricane katrina: status and issues", (Congressional Information Service, Library of Congress, 2005).

Serrano, M. A. and M. Boguná, "Topology of the world trade web", Physical Review E **68**, 1, 015101 (2003).

Shen-Orr, S. S., R. Milo, S. Mangan and U. Alon, "Network motifs in the transcriptional regulation network of escherichia coli", Nature genetics **31**, 1, 64–68 (2002).

Shneiderman, B., "The eyes have it: A task by data type taxonomy for information visualizations", in "Visual Languages, 1996. Proceedings., IEEE Symposium on", pp. 336–343 (IEEE, 1996).

Shneiderman, B. and A. Aris, "Network visualization by semantic substrates", IEEE Transactions on Visualization and Computer Graphics **12**, 5, 733–740 (2006).

Shutters, S. T. and R. Muneepeerakul, "Agricultural trade networks and patterns of economic development", PloS one **7**, 7, e39756 (2012).

Silberglitt, R., *Critical Materials, US Import Dependence, and Recommended Actions* (RAND Corporation, 2015).

Squartini, T. and D. Garlaschelli, "Triadic motifs and dyadic self-organization in the world trade network", in "International Workshop on Self-Organizing Systems", pp. 24–35 (Springer, 2012).

Sternberg, T., "Chinese drought, bread and the Arab Spring", Applied Geography **34**, 519–524 (2012).

Stocker, T. F., D. Qin, G.-K. Plattner, M. Tignor, S. K. Allen, J. Boschung, A. Nauels, Y. Xia, V. Bex and P. M. Midgley, "Climate change 2013: The physical science basis. contribution of working group i to the fifth assessment report of the intergovernmental panel on climate change, 1535 pp", (2013).

Stouffer, D. B., M. Sales-Pardo, M. I. Sirer and J. Bascompte, "Evolutionary conservation of species' roles in food webs", Science **335**, 6075, 1489–1492 (2012).

Sun, G.-D., Y.-C. Wu, R.-H. Liang and S.-X. Liu, "A survey of visual analytics techniques and applications: State-of-the-art research and future challenges", Journal of Computer Science and Technology **28**, 5, 852–867 (2013).

Timmer, C. P., "Reflections on food crises past", Food policy **35**, 1, 1–11 (2010).

Trenberth, K., "Uncertainty in hurricanes and global warming", Science **308**, 5729, 1753–1754 (2005).

UNDESA, "The global food crises", The Report on the World Social Situation 2011: The Global Social Crisis (2011).

Webster, P. J., G. J. Holland, J. A. Curry and H.-R. Chang, "Changes in tropical cyclone number, duration, and intensity in a warming environment", Science **309**, 5742, 1844–1846 (2005).

Winkler, M. and J. Reichardt, "Motifs in triadic random graphs based on steiner triple systems", Physical Review E **88**, 2, 022805 (2013).

Zhou, M., G. Wu and H. Xu, "Structure and formation of top networks in international trade, 2001–2010", Social Networks **44**, 9–21 (2016).